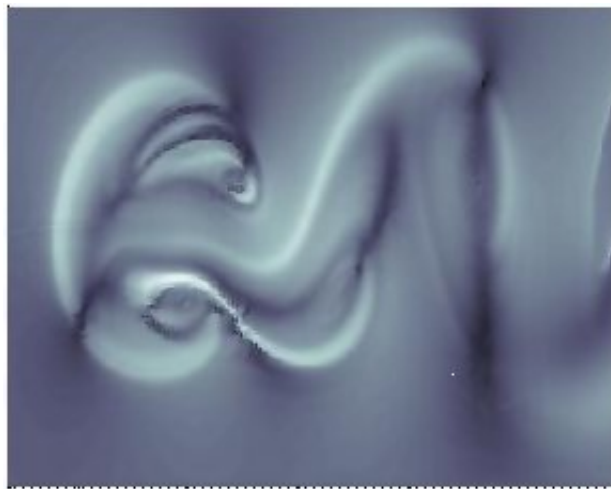# Methods for Vortex Identification

Vivianne Holmén

December 7th 2012

Abstract

Initially, this paper presents an overview of the existing methods used for the identification of vortices in fluids, attempting to point out their different strengths and weaknesses. In addition, a new method is proposed to identify vortices directly from velocity field information. It defines a point inside a vortex as a point around which there is rotation. By looking at the velocity directions in the neighbourhood of a point we decide if there is rotation. A measure of the strength of rotation at the point is also introduced based on the magnitude of the velocity components in the neighbourhood. The method is tested on simulated data and performs well. Finally a Lagrangian identification method (Direct Lyapunov Exponents, DLE) is used to attempt to calibrate the λ_2-criterion in order to match an objectively defined edge. The results here indicate that it might not be possible to find a λ_2 threshold to match edges found using the DLE method.

.

Contents

4

1 Introduction

While we all may believe we know how to recognise a vortex, a mathematically unambiguous definition is hard to find. The difficulty lies in that our intuitive concept of a vortex can be described as a vaguely circular motion in a fluid. The problem is exacerbated by the lack of clear edges to a vortex, i.e. when looking at a vortex as a finite structure it is difficult to agree on where the vortex ends.

Since the discovery of vortical structures in turbulence, research in the area of vortex identification has been of interest. It has resulted in an array of methods designed to identify vortices given the output of simulations or velocity measurements in experiments. While some of these methods have become very popular and are widely used in fluid dynamics, the λ_2 method presented in [11] being most notable, it is still not universally accepted. A further complication is the visualisation of the results given by different methods. For example, some methods introduce different thresholds for visualisation purposes, varying the thresholds can greatly change the appearance of the results.

Identification of vortices can be seen as a tool for understanding complex flow phenomena. For example, being able to follow individual vortices in a turbulent flow throughout their lifetimes. The methods developed are therefore an important aid for research in fluid dynamics. Furthermore, they have a practical application in industry. The successful control of flows requires an accurate understanding of the structures present in the fluid. For example, in combustion engines it is interesting to control the surface area of the flame front in order to optimise the combustion reactions. In this case vortices can both improve the reaction by mixing fuel and air and have a negative effect, for example if the vortices are too large they might distort the flame front too much.

The aim with this thesis is to study the difficulties in defining, identifying and visualising vortical structures. This is accomplished by investigating existing methods for vortex identification and suggesting a new method based on a simple analysis of the velocity field. A comparison of the results given by different methods is of interest. The problems surrounding the visualisation of the results are to be addressed by suggesting different possible ways to show the vortices in an image. This is especially interesting when looking at three-dimensional data. Finally we combine two methods in order to attempt to exploit the strengths of each method and provide a more complete understanding of the magnitude and behaviour of vortices.

There are two distinct problems: the identification of vortices, and the visualisation of the results. In complex flows there are many interacting vortices, all which may be bent or twisted resulting in rotation in several different planes for each single vortex; therefore, even assuming a method of identification is agreed upon, displaying the results in an easily understood format is still a difficult task.

The methods implemented for this Master's thesis have been programmed in Matlab.

1.1 Structure of the Thesis

This Master's thesis is structured so that a short presentation of theoretical concepts relevant to the results is given first. The theory section includes some

basic concepts of fluid dynamics and a qualitative description of how a vortex may be formed in a simple case. Each flow case that was studied with our vortex identification method is described here, including how and where we expect to find the vortices in each case.

Furthermore, the theory section includes an introduction to some of the mathematical formalia encountered in the different identification methods presented. That section aims to provide a basic background that will allow the reader to easily follow the theory behind the methods. It includes tensors and lagrangian frames of reference, especially in connection to Lyapunov exponents and other ideas from dynamic systems theory.

The second section goes through the different methods that have been used, and still are used, for identifying vortices. It is not exhaustive, but it shows a broad spectrum of the ideas that have been attempted and gives a clear idea as to what aspects of the flow are viewed as central when discussing vortices. At the end of the section a summary of the methods, with references to the publications where they have been presented, is given. Some of the strengths and weaknesses, as presented by different researchers, of the different methods are also included in this summary.

The third section presents the first identification method implemented for this Master's thesis. It is validated by being applied to the data sets described earlier, and further compared to one of the more popular identification methods (λ_2-method). The results are shown with a short discussion for each data set, especially in relation to the variables changed.

The fourth section describes a method that attempts to combine two of the methods presented in Section 2. The method itself and results, including a discussion, is presented there.

The final section has conclusions regarding both methods developed in this thesis and potential future works.

2 Theory

2.1 Fluid Dynamics

Fluid mechanics is a discipline in applied mechanics concerned with the behaviour of liquids and gases at rest or in motion. Fluid dynamics is the part that is concerned with the motion of fluids. Among other things, fluid dynamics tries to describe how the fluid flow evolves under complex dynamics which may involve heat transfer and possibly chemical reactions, as for example in combusting flows.

The physical characteristics of fluid motion are usually described through fundamental mathematical equations. Most of the behaviour of fluids in motion can be described by a number of partial differential equations known as **the Navier-Stokes equations**. These equations describe the basic physical laws that govern the motion of the fluid. While these equations may seem simple the solutions differ greatly in character depending on the starting conditions and the characteristics of the fluid.

Flow is generally divided into different groups depending on the properties of the fluid particles in the flow. A very important distinction is whether a flow is *laminar* or *turbulent*. The Reynolds number, defined below, is used to

distinguish between laminar and turbulent flow. Low Reynolds numbers are associated with laminar flows, and large ones with turbulent flows. There is also a transitional flow, which describes the case when laminar flow is becoming turbulent but is not yet fully turbulent. Both laminar and turbulent flows are generaly unsteady, meaning that the velocity at a given point in space varies with time. A flow is steady if there is no change in the velocity field through time. Therefore it is not possible to have a steady turbulent flow. Turbulent flow is generally seen as chaotic as there is no regular variation or identifiable pattern in the unsteadiness of turbulence. Laminar flow, on the other hand, can be steady but is not necessarilly so.

The Reynolds number is a non-dimensional ratio between the inertial force and the viscous forces acting on the fluid. The Reynolds number is defined as $Re = \frac{\rho V l}{\mu}$, where ρ is the fluid density, V is the velocity of the fluid, l is a characteristic length and μ is the viscosity of the fluid. The exact values for when Reynolds numbers are "large" or "small" are not well-defined but change depending on the actual problem. For example the flow in a round pipe is considered laminar if Re is less than approximately 2100, and turbulent for values greater than 4000 [20].

Viscosity is a property specific to each fluid and can be seen as a measure of how easily the fluid flows. The *dynamic viscosity*, μ, of a fluid is the constant of proportionality in the relationship

$$\tau = \mu \frac{du}{dy}$$

which relates the shearing stress to the rate of shearing strain in a fluid. Viscosity is very sensitive to temperature, but not to pressure. It is often combined with density in fluid flow problems, and is then called the *kinematic viscosity* $\nu = \frac{\mu}{\rho}$. A large value of viscosity means the fluid is less likely to flow, i.e. the forces between the particles in the fluid are large enough to withstand external forces without moving too much.

2.1.1 Vortices and Coherent Structures

Both vortices and coherent structures lack a strict definition. In general any form of pattern arising in the flow that has an effect on transport is considered a coherent structure. However, when talking about vortices people have a general understanding of what is meant: existence of some form of common particle rotation. The typical intuitive vortex is a tornado, or maelstrom. However, while this is generally accepted it is more difficult to reach a consensus regarding how far away from a centre of rotation a vortex actually extends. Due to viscosity there is no clear start or end to the structure. This is further complicated when there are several structures interacting with each other. Vortices are commonly associated with turbulence, but they occur in laminar flow as well.

A coherent structure (CS) is an idea that was orginally introduced when discussing turbulence. It singles out areas in the fluid where there is less mixing or movement than would be otherwise expected considering the velocity field, that means that a section of the fluid remains roughly together (coherent) while moving in the fluid.

Both these concepts, however, are vague and not strictly defined. Comparing the two descriptions of coherent structures below we can see that they are both

vague. A major difference is that while one expects vortical motions the other does not require this.

"It is generally accepted that flows with general time dependence admit emergent patterns which influence the transport of tracers, those structures are often generically refered to as Coherent Structures" [18].

"Turbulent shear flows have been found to be dominated by spatially coherent, temporally evolving vortical motions, popularly called coherent structures" [11].

Vortices are coherent structures, and while the inverse is generally true, it is not necessarily so.

2.1.2 Lagrangian Coherent Structures

The distinction between a CS and a Lagrangian coherent structure (LCS) is mainly in the nature of the methods used to identify them."A Lagrangian Coherent Structure is basically a coherent structure that is identified using methods that work in the Lagrangian frame, that is then the CS are studied in terms derived from fluid trajectories" [18]. Unambiguous definitions depend on which method is being used to find them, see the Overview of Methods section.

LCS are separated into two groups, connected to their definitions from dynamical systems: attracting and repelling structures. This has to do with whether fluid particles that get close to the structure will be pulled into it or pushed away. Intuitively, this places vortices in the former group, since particles are pulled into the vortical motion.

Mixing in the fluid is also determined by the interplay of LCS. The edges of an LCS are generally material lines in two dimensions (or surfaces in three-dimensional space), meaning that there is no flux through the edges. Therefore LCS result in a partitioning of the fluid. "Lagrangian coherent structures typically represent separatrices which divide the flow into dynamically distinct regions" [18]. The idea of finding lines that separate dynamically distinct regions can of course be used to try to find the edges of a vortex. The dynamics of the fluid are different inside the vortical structure from the rest of the flow.

2.1.3 Example of Vortex Formation in the Wake of a Cylinder

A group of vortices that are easy to identify and visualise are the ones formed in the wake of a cylinder. If the cylinder can be seen as infinite (meaning there will be no influence in our data from the ends of the cylinder) the flow pattern will be practically two-dimensional, allowing us to look at only a plane. By varying the velocity of the fluid passing by the cylinder different Reynolds numbers are attained, and therefore different behaviours can be observed in the wake of the cylinder.

At low Reynolds numbers viscous effects dominate the behaviour of the fluid and the flow therefore follows the edges of the cylinder all the way through. This type of flow is also known as creeping flow. The streamlines in this case will be symmetric before and after the cylinder. There is no wake to speak of.

By increasing the Reynolds number, the region where viscous effects dominate becomes smaller, only extending a short distance ahead of the cylinder. The viscous effects are convected downstream and the flow loses its symmetry. The flow also separates from the cylinder, creating the wake of the cylinder.

Depending on the Reynolds number any of the cases shown in Figure 2 can be observed.

The velocity of the fluid decreases as it gets close to the cylinder until it reaches zero, at the so-called *stagnation point*, point (1) see Figure 1. As the fluid then moves along the side of the cylinder to point (2) its velocity increases until it reaches a maximum. After point (2) the velocity decreases again until at point (3) it separates from the edge of the cylinder. The exact position of point (3) depends on the characteristics of the flow. At very low Reynolds numbers separation does not occur, see Figure 2.
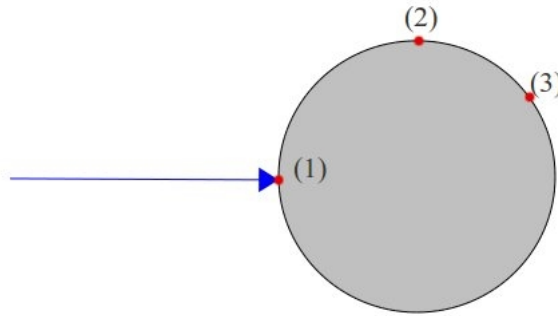

Figure 1: Different points of interest along the edge of the cylinder.

The velocity of the fluid beyond the separation point is lower than that of the freestream, this velocity difference will force a rotation as the faster fluid overtakes the slower one. Eventually a backflow occurs in the separation area, causing vortices. If the Reynolds number is high enough the vortices are shed from the cylinder.

2.1.4 The Simulated Data Sets used throughout the Report

The data used in this thesis is the result of simulation of different cases. It was all provided by my supervisor. Here the different simulations will be described, including what we expect to find in each case.

1. Laminar flow after an infinite cylinder set along the y-axis. The flow direction is the z-direction. Reynolds number is 100. The vortices formed in the wake are essentially 2-dimensional in character with rotation in the xz-plane. The vortices are shed alternately from either side of the cylinder, with opposite rotation. This is the case described as an example in the previous section. Data for this case exists in both a coarse and a fine grid.

2. Laminar flow after a spherical object. The flow is in the z-direction. Reynolds number is 400. This results in highly three-dimensional vortices, i.e. a single vortex has many planes of rotation and it is bent like
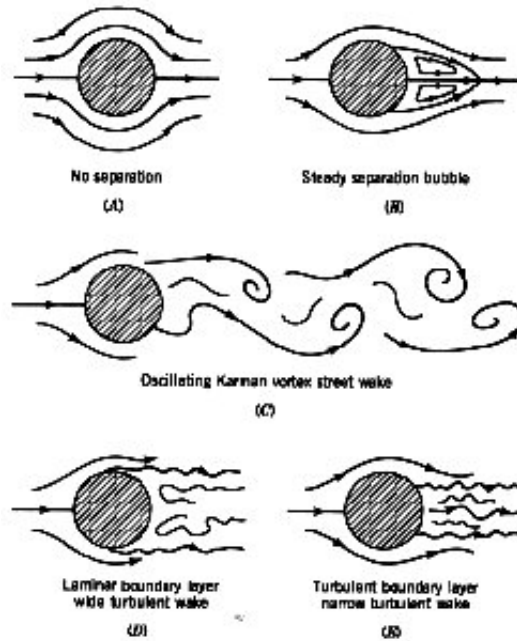
Figure 2: Diagram of the different flow patterns that can be found in the wake of a circular cylinder [20].

master thesis

   a "hairpin". They are however well defined as this is still a laminar case due to its low Reynolds number.

3. Turbulent flow after a spherical object. This is the same case as the previous one, except at a much higher Reynolds number, 10000, which means that the wake is turbulent. This means that the vortices will be less organised, more of them, and often smaller.

4. A jet. The flow in a jet is turbulent.

2.2 Tensors

Cartesian tensors are necessary when representing quantities with several directions associated with them. A pth-order tensor has p directions associated with it, and 3^p components when working in three-dimensional space. Using the Einstein summation convention simplifies the notation associated with Cartesian tensors. Using this convention if a suffix is repeated then summation over all values of the suffix is implied. An important rule of the summation convention is that a suffix cannot appear more than twice in an expression.

   Tensors were introduced to relate observations made in different frames of reference to each other. Orthogonal transformations of the type

$$\mathbf{X} = \mathbf{Q}\mathbf{x} + \mathbf{B} \qquad (1)$$

10

where $\mathbf{Q}$ is an orthogonal matrix, leave the distance between two points invariant.

Bearing this in mind a *tensor of second order* is defined as a quantity with physical dimension, characterised by n^2 real numbers (n being the physical dimension of space) such that under a change of reference frame, given by (1), the relation (below) between the components a_{ij} and A_{KJ} in the two frames is satisfied.

$$A_{KJ} = Q_{Kk}Q_{Jj}a_{kj}, K, J = 1, 2, ..., n$$

It is important to note that the **order** of a tensor relates to the directions associatied with it, while the **physical dimension** has to do with the dimensions of the Euclidean space we are working in. For most physical applications this is equivalent to 3-dimensional space [1].

2.2.1   Structural Properties of Tensors

A tensor is called **symmetric** with respect to the indices k_i and k_j, $i < j$, if these indices can be interchanged, without the corresponding components changing their values.

In contrast, a tensor is called **antisymmetric** (or skew-symmetric) with respect to the indices k_i and k_j, $i < j$, if by interchanging the indices k_i and k_j the corresponding components change their sign.

Both definitions are valid in any reference frame, which entails that these properties have an invariant character and therefore express objective properties of the physical quantities represented by the tensors [1].

2.3   Eulerian and Lagrangian Fields

Eulerian fields are indexed by the position $\bar{x}$ in an inertial field. The vector fields we are used to working with are Eulerian, i.e. velocity field, pressure field, density field.

In the Lagrangian frames a **fluid particle** is defined as a point that moves with the local fluid velocity. In this case $\mathbf{X}^+(t, \mathbf{Y})$ denotes the position at time t of the fluid particle that is located at $\mathbf{Y}$ at the specified fixed reference time t_0. Mathematically this can be written:

$$\mathbf{X}^+(t_0, \mathbf{Y}) = \mathbf{Y}$$

where $\mathbf{X}^+$ determines the position of the fluid particle at the reference time, t_0 and the following describes the fluid particle moving with the local fluid velocity.

$$\frac{\partial}{\partial t}\mathbf{X}^+(t, \mathbf{Y}) = \mathbf{U}(\mathbf{X}^+(t, \mathbf{Y}), t)$$

This definition is given in terms of the Eulerian velocity field, $\mathbf{U}$, for any $\mathbf{Y}$. The equation can be integrated backward and forward in time to obtain $\mathbf{X}^+(t, \mathbf{Y})$ for all t.

Lagrangian fields are indexed by the position $\mathbf{Y}$ at reference time t_0 and not by the current position of the fluid particle. $\mathbf{Y}$ is called the *Lagrangian coordinate* for fixed $\mathbf{Y}$.

A fluid particle is also called a *material point.* Similarly one can define material lines, surfaces and volumes. For instance, at time t_0 a simple closed surface S_0 encloses the volume V_0. The corresponding *material surface* $S(t)$ is defined to be coincident with S_0 at time t_0. Every point in $S(t)$ moves with the local fluid velocity. Because a material surface moves with the fluid, the relative velocity between the surface and the fluid is zero. Therefore a fluid particle cannot cross a material surface, i.e. there is no mass flux accross the surface [17].

2.4   Dynamical Systems

A *dynamical system* on a topological space X is a continuous map $\Phi : G \times X \to X$ such that, for all $x \in X$ and for all $s, t \in G$,

$$\Phi(s + t, x) = \Phi(s, \Phi(t, x))$$

$$\Phi(0, x) = x.$$

If a systems past and future states can be completely determined by its state at any one particular instant the process is deterministic. The possible states of the system in which the process is taking place may be represented by points of a differentiable manifold, known as the state space of the model. A deterministic process is often governed by a smooth vector field on the state space, the dimension of the space depends on the process being studied. In fluid dynamics, for example, we must take into account the velocity of the fluid at infinitely many different points implying that the state space is infinite dimensional [10]. A simulated flow however has a finite dimensional state space as velocity information is only known at the grid points.

The Lyapunov exponents of a transformation $\Phi : X \to X$ are a measure of the local expansion or contraction properties of Φ. Lyapunov exponents are defined by a limit process, but can be approximated numerically. The method can only be used for smooth dynamical systems since they require a differentiable structure. The idea behind Lyapunov exponents can be explained as follows: Let X carry a differentiable structure, and let Φ be differentiable. For each tangent vector $\mathbf{V}$ at some $x \in X$, we consider the iterated application of the derivative $d\Phi$ of Φ on $\mathbf{V}$:

$$d\Phi^n(x)(\mathbf{V}),$$

determine its norm in a given metric on X and let n tend to ∞ [12].

Under the assumption that Φ is ergodic, there are at most $d = dimX$ different possibilites for the corresponding limits

$$\lambda(x) = \lim_{n \to \infty} \frac{1}{n} \ln \|d\Phi^n(x)(V)\| \tag{2}$$

These limits are called the Lyapunov exponents of Φ, and they do not depend on the measure nor on the metric employed [12]. In the context of fluid dynamics the Cauchy-Green deformation tensor is used instead of the iterated derivative of Φ on V. It is also generally interesting to only look at the largest Lyapunov exponent, related to the largest eigenvalue of the deformation tensor, and therefore the direction in which expansion or contraction is the greatest.

A linear map is hyperbolic if it has no eigenvalues on the unit circle. For a point to belong to both a stable and an unstable set it must be hyperbolic. Stability of manifolds relates to whether they are attracting or repelling structures. Repelling structures emerge under forward integration, while the attracting ones require backward integration. Attracting Lagrangian coherent structures are unstable manifolds for time-independent vector fields. Repelling LCS are the stable manifold in the same vector fields [5].

3 Overview of Methods

3.1 Methods Based on the Velocity Gradient tensor

The velocity gradient tensor $\bar{D}$ can be written as $D_{ij} = \frac{\partial u_i}{\partial x_j}$. As this is a second order tensor it can be decomposed into a symmetric and a skew-symmetric part $D_{ij} = S_{ij} + \Omega_{ij}$ where $S_{ij} = \frac{1}{2}\left(\frac{\partial u_i}{\partial x_j} + \frac{\partial u_j}{\partial x_i}\right)$ and $\Omega_{ij} = \frac{1}{2}\left(\frac{\partial u_i}{\partial x_j} - \frac{\partial u_j}{\partial x_i}\right)$. S_{ij} is known as the rate-of-strain tensor, and Ω_{ij} is the vorticity tensor.

The charateristic equation for ∇u is given by

$$\lambda^3 + P\lambda^2 + Q\lambda + R = 0$$

where P, Q and R are the three invariants of the velocity gradient tensor. Using the decomposition into symmetric and anti-symmetric parts these invariants can be expressed as follows.

$$P = -tr(\bar{D})$$

$$Q = \frac{1}{2}(tr(\bar{D})^2 - tr(\bar{D}^2)) = \frac{1}{2}||\bar{\Omega}||^2 - ||\bar{S}||^2$$

$$R = -det(\bar{D})$$

3.1.1 Q-criterion

The **Q-criterion** defines a vortex as a "connected fluid region with a positive second invariant of ∇u"[14], i.e $Q > 0$. This criterion also adds a secondary condition on the pressure, requiring it to be lower than ambient pressure in the vortex. Looking at the definition of the second invariant we can see that Q represents the local balance between shear strain rate and vorticity magnitude, defining vortices as areas where the vorticity magnitude is greater than the magnitude of rate-of-strain [9, 14].

3.1.2 Δ-criterion

The **Δ-criterion** defines vortices as "regions in which two of the eigenvalues of ∇u are complex and the streamline pattern is spiralling or closed"[14]. In order to determine if the eigenvalues are complex we examine the discriminant of the characteristic equation.

$$\Delta = \left(\frac{Q}{3}\right)^3 + \left(\frac{R}{2}\right)^2 > 0$$

This definition is valid for incompressible flows where $P = 0$. The streamlines are closed or spiralling if two of the eigenvalues form a complex conjugate pair. By looking at the Δ we can see that $Q > 0$ is a more restrictive criterion than $\Delta > 0$ [2].

3.1.3 λ_2-criterion

The λ_2-**criterion** looks for a pressure minimum but removes the effects from unsteady straining and viscosity by discarding these terms. Taking the gradient of the Navier-Stokes equations results in

$$a_{i,j} = -\frac{1}{\rho}p_{ij} + \nu u_{i,jkk}$$

where a_{ij} is the acceleration gradient and p_{ij} is symmetric. Decomposing the acceleration gradient into symmetric and antisymmetric parts we get the vorticity transport equation as the antisymmetric part, and the symmetric part

$$\frac{DS_{ij}}{Dt} - \nu S_{ij,kk} + \Omega_{ik}\Omega_{kj} + S_{ik}S_{kj} = -\frac{1}{\rho}p_{ij}$$

The first two terms in the left hand side represent unsteady irrotational straining and viscous effects respectively. Therefore only $S^2 + \Omega^2$ is considered to determine if there is a local pressure minimum that entails a vortex. A vortex is defined as "a connected region with two negative eigenvalues of $S^2 + \Omega^2$" [11]. Since $S^2 + \Omega^2$ is symmetric it has real eigenvalues only, and by ordering the eigenvalues $\lambda_1 \leq \lambda_2 \leq \lambda_3$ the definition becomes equivalent to requiring that $\lambda_2 < 0$. Generally visualised as isosurfaces for different values of $-\lambda_2$ [11].

In planar flows, the three conditions described above are equivalent.

3.1.4 Swirling Strength Criterion

The **Swirling Strength Criterion** uses the imaginary part of the complex eigenvalues of the velocity gradient tensor to visualise vortices. It is based on the idea that the velocity gradient tensor in Cartesian coordinates can be decomposed as

$$\nabla u = [d_i j] = [\bar{\nu}_r \; \bar{\nu}_{cr} \; \bar{\nu}_{ci}] \begin{bmatrix} \lambda_r & 0 & 0 \\ 0 & \lambda_{cr} & \lambda_{ci} \\ 0 & -\lambda_{ci} & \lambda_{cr} \end{bmatrix} [\bar{\nu}_r \; \bar{\nu}_{cr} \; \bar{\nu}_{ci}]^T$$

where λ_r is the real eigenvalue with corresponding eigenvector $\bar{\nu}_r$ and the complex conjugate pair of complex eigenvalues is $\lambda_{cr} \pm i\lambda_{ci}$ with corresponding eigenvectors $\bar{\nu}_{cr} \pm i\bar{\nu}_{ci}$. By expressing the local streamlines in a coordinate system spanned by the three vectors $(\bar{\nu}_r, \bar{\nu}_{cr}, \bar{\nu}_{ci})$ we can see that the local flow is either stretched or compressed along the axis $\bar{\nu}_r$ while on the plane spanned by the vectors $\bar{\nu}_{cr}$ and $\bar{\nu}_{ci}$ the flow is swirling. The strength of this swirling motion can be quantified by λ_{ci}, called the local swirling strength of the vortex. The threshold for λ_{ci} is not well-defined. On theoretical grounds it should be set to zero, but the results are smoother when it is set to a positive value. The criterion is therefore $\lambda_{ci} \geq \epsilon > 0$ [21].

3.1.5   Enhanced Swirling Strength Criterion

The **Enhanced Swirling strength criterion** uses the idea presented by [4] regarding the non-local aspects of vortical structures. The idea is to approximate the non-local concept or orbital compactness based on local analysis of time-frozen flow fields. By looking at the projected motion of a fluid particle in the swirling plane (as seen in the swirling strength criterion) it can be shown that the time period for one revolution in the vortex plane is $2\pi/\lambda_{ci}$. Two points in this plane with an initial separation of r_0 will be separated by r_f after n revolutions. The two distances can be expressed in terms of the eigenvalues of ∇u as

$$\frac{r_0}{r_f} = \exp\left(2\pi n \frac{\lambda_{cr}}{\lambda_{ci}}\right).$$

The ratio $\lambda_{cr}/\lambda_{ci}$ is called the inverse spiralling compactness, which is used to approximate the orbital compactness in a vortex. The added advantage of using this method is to restrict regions of strong outward spiralling motion in the definition. A vortex is therefore defined as regions where $\lambda_{ci} \geq \epsilon$ and $\lambda_{cr}/\lambda_{ci} \leq \delta$ where ϵ and δ are positive thresholds [2].

3.1.6   Triple Decomposition

The idea behind introducing a triple decomposition of the velocity gradient tensor is to try to extract a so-called **pure swirling motion**. It is motivated by the fact that vorticity cannot distinguish between shearing motion and swirling motion. The aim is to decompose an arbitrary instantaneous state of the relative motion into three elementary motions:

1. Pure Shearing (Elongation)

2. Rigid body rotation

3. Irrotational straining (Shearing)

The three motions are described in terms of a structured continuum where groups of material particles form fluid elements. The relative motion of the particles then result in different motions and deformation of the fluid element. The velocity gradient tensor is broken down into three additive elements, all with tensor characterisics, as follows,

$$\nabla \bar{u} = (\nabla \bar{u})_{EL} + (\nabla \bar{u})_{RR} + (\nabla \bar{u})_{SH}$$

where the terms correspond to each of the elementary motions. The elongation tensor should be symmetric, the rigid body rotation tensor antisymmetric and the shearing tensor purely asymmetric. The requirement of having a purely asymmetric tensor means that a suitable frame of reference has to be chosen. The procedure to attain an unambiguous decomposition algorithm can be described by the three steps below.

Begin by finding the *basic reference frame* (BRF) defined by the condition

$$[|S_{12}\Omega_{12}| + |S_{23}\Omega_{23}| + |S_{31}\Omega_{31}|]^{BRF}$$

$$= MAX[|S_{12}\Omega_{12}| + |S_{23}\Omega_{23}| + |S_{31}\Omega_{31}|]^{ALLFRAMES}.$$

in this frame the velocity gradient is decomposed as follows

$$\nabla u \equiv \begin{bmatrix} u_x & u_y & u_z \\ v_x & v_y & v_z \\ w_x & w_y & w_z \end{bmatrix} = \begin{pmatrix} residual \\ tensor \end{pmatrix} + \begin{pmatrix} shear \\ tensor \end{pmatrix}$$

where the residual tensor is given by

$$\begin{pmatrix} residual \\ tensor \end{pmatrix} = \begin{pmatrix} u_x & (sgnu_y)MIN(|u_y|,|v_x|) & \bullet \\ (sgnv_x)MIN(|u_y|,|v_x|) & v_y & \bullet \\ \bullet & \bullet & w_z \end{pmatrix}$$

where the two non-specified off-diagonal elements are calculated in the same way as the other two off-diagonal elements are. Finally the residual tensor is decomposed into its symmetric and antisymmetric parts, which then correspond to ∇u_{EL} and ∇u_{RR}. The last step is to transform the results back to the original refence frame.

This method then defines a vortex as a connected fluid region with a non-zero magnitude of the *residual* vorticity, the antisymmetric part of the residual tensor. The method is only described for planar flows, so its effectiveness in three-dimensional vortex identification is not clear [14].

3.2 Vorticity

Vorticity is defined as the curl of the velocity, $\omega = \nabla \times \mathbf{U}$ and it is equal to twice the rotation of the fluid at $(\mathbf{x}, t)$. As a result of this, the vorticity can be used directly to identify vortices. A problem associated with this method is that vorticity cannot distinguish between swirling motions and shearing motions [13].

Vorticity can be readily visualised by plotting isosurfaces of $|\omega|$. This can be problematic however as different thresholds can result in different geometrical structures. Also, if the velocity gradient acts to stretch the material line element aligned with ω, then $|\omega|$ increases correspondingly. This is known as vortex stretching, which means that as a vortex is stretched along the velocity gradient, the magnitude of vorticity will increase. This effect does not exist for two-dimensional flows.

Vorticity is a vector field and therefore has integral curves obtained by solving

$$\frac{d\mathbf{x}}{ds} = \frac{\omega}{|\omega|}$$

where s is the distance along the vortex line. Other parameters can be used instead of s, and scaling with the magnitude of vorticity is not necessary. Infinitely many vortex lines can be drawn in the flow, therefore in order to get useful results using this method, the choice of starting point is very important. If the starting point is not a part of an organised structure there is a risk that its motion will be erratic, resulting in lines that traverse the entire flow without any clearly visible pattern. Therefore, the structures to be visualised have to be identified before drawing the lines. This is therefore a method for *visualising* vortices, not identifying them [16, 13].

16

3.3   Lagrangian Methods

3.3.1   Direct Lyapunov Exponent

The Lyapunov exponent (to be defined below) at a given point provides a measure of the separation of neighbouring particle trajectories initialised near that point. That is, a particle located at position $\mathbf{x}_0$ at time t_0 will have position given by $\mathbf{x}(t, \mathbf{x}_0, t_0)$ at time t. An expansion coefficient related to the evolution of the particle can be calculated by looking at the finite-time version of the (right) Cauchy-Green deformation tensor

$$\Delta = \frac{d\phi_{t_0}^t(\mathbf{x})}{d\mathbf{x}}^T \frac{d\phi_{t_0}^t(\mathbf{x})}{d\mathbf{x}}$$

and using its largest singular value $\lambda_{max}\Delta$. Since the maximum eigenvalue is used in this definition, there is no direction information in the Lyapunov exponent.

The (largest) direct Lyapunov exponent can be defined in different ways as the two examples below show

$$\sigma_T = \frac{1}{|T|} ln \sqrt{\lambda_{max}(\Delta)} \quad [18],$$

$$\sigma_T = \frac{1}{2T} ln(\lambda_{max}(\Delta)) \quad [6].$$

Regions of maximum material stretching (hyperbolic Lagrangian Coherent Structures, LCS) generate maximising curves for the DLE field, known as ridges. However, maximising curves of the DLE field are not necessarily regions of maximum material stretching, they can also indicate locally maximal shear. To make sure that a ridge is indeed a hyperbolic LCS, the strain rate normal to the ridge can be calculated. Forward and backward time integrations also provide different information, backward time integration reveals attracting material lines, while forward time integration ridges mark the location of repelling material lines [6].

3.3.2 M_Z-criterion

This method is objective, meaning that it remains invariant under coordinate changes of the form

$$\bar{\mathbf{x}} = \mathbf{Q}(t)\mathbf{x} + \mathbf{b}(t)$$

where $\mathbf{Q}(t)$ is a time-dependent proper orthogonal tensor, and $\mathbf{b}(t)$ is a translation vector [8]. This allows for having rotating frames of reference, which can be interesting when looking at the structures in a fluid inside a rotating tank for example.

The M_Z-criterion describes vortices through the stability of fluid trajectories in three-dimensional incompressible flows. Physically, it defines a vortex as a material region where an element's long-term evolution does not follow the trend expected from the instantaneous rate-of-strain tensor.

The rate of strain acceleration tensor is defined as

$$\mathbf{M} = \partial_t \mathbf{S} + (\nabla \mathbf{S})\mathbf{v} + \mathbf{S}(\nabla \mathbf{v}) + (\nabla \mathbf{v})^T \mathbf{S}$$

where $\mathbf{S}$ is the rate of strain tensor.

The restriction to a zero-strain cone Z that travels with the trajectory, M_Z, remains positive definite if the trajectory is hyperbolic.

Trajectories in regions of sustained material stretching and folding have a stabilty type known as Lagrangian hyperbolicity. This method relates Lagrangian hyperbolicity to the Eulerian domain, by showing that stability can be guaranteed if the trajectory remains in a hyperbolic domain of the Eulerian frame. In order to find this type of stability three-dimensional space is partitioned into hyperbolic and elliptic domains, where the *hyperbolic domain* $H(t)$ is the set of points at which $\mathbf{M}_Z$ is positive definite. The *elliptic domain* is the set of points at which $\mathbf{M}_Z$ is indefinite. They are both three-dimensional open sets separated by two-dimensional boundaries.

In the *hyperbolic domain* material elements align with subspaces that are close to the eigenvectors of positive strain, while in the *elliptic domain* material alignment is either absent or inconsistent with the trend suggested by the eigenvalues of the rate of strain.

A vortex is defined to be a bounded and connected set of fluid trajectories that remain in the elliptic region $E(t)$, thereby avoiding the hyperbolic domain. That is, a vortex is a set of fluid trajectories along which $\mathbf{M}_Z$ is indefinite [8].

3.4 Other Methods

3.4.1 R-definition

This method attempts to add a concept of non-locality to the identification of vortices, thereby adding the idea of vortices as structures. It is a Galilean invariant method that uses the notion that the particles inside a vortical structure show small variations in their relative distance even when following completely different trajectories.

Let us consider two particles in a flow (a, b) and their respective velocities $\mathbf{u_a}$ and $\mathbf{u_b}$. Then the ratio

$$R(\mathbf{x}, t) = \frac{|\int\limits_0^t \mathbf{u_a}(\tau)d\tau - \int\limits_0^t \mathbf{u_b}(\tau)d\tau|}{\int\limits_0^t |\mathbf{u_a}(\tau) - \mathbf{u_b}(\tau)|d\tau}$$

measures the difference in the total distance travelled by each particle (the particle trajectories) and the relative distance between them. The ratio is bounded between 0 and 1, and assumes lower values for pairs of particles belonging to a vortical structure.

This method is practically applied by selecting a large number of particles at random positions in a flow field. These particles are then split up into pairs where any one particle can be a part of more than one pair. The starting distance between the two particles in each pair should be within a previously defined interval $[d_m, d_M]$. This interval can be chosen freely and therefore serves as a filtering tool, by setting a lower limit. The structures with a spacial scale smaller than d_m will not be considered in the results.

The parameter t can be viewed as a pseudo-time, allowing this analysis to be made for flows frozen at a certain point in time. The choice of this parameter

is not crucial, but when it is chosen it is important to observe that if t is too high some information can be lost.

The ratio $R(t)$ is then calculated for every pair and followed in pseudo-time by integrating the equation describing its trajectory, $\frac{d\mathbf{x}}{dt} = \mathbf{u}(\mathbf{x}, t)$. The results can then be plotted on a graph by choosing a threshold value R_{th} and plotting in the flow field the midpoint of pairs of particles with $R(t) \leq R_{th}$ at the instant $t = 0$ [4].

3.4.2 Closed or Spiralling Streamlines

The use of spiralling or closed pathlines or streamlines to detect vortices is intuitive. It is also a non-local method, as it looks at the trajectories of several particles in relation to one another. However it is not Galilean invariant, this means that different results are received if the frame of reference is translated. This method is difficult to apply in complex flows due to their rapidly transforming vortex topology [11].

3.4.3 Pressure Minima

When looking at a steady inviscid planar two-dimensional flow, a pressure minimum can be found at the center of a rotating motion. This is a consequence of the balance of the forces acting on a fluid element in the radial direction. Based on this, a pressure minimum has been used as an indicator for rotation in a fluid, i.e. a vortex. However, the argument for pressure minima no longer applies when the flow is unsteady, viscous or three-dimensional. While it is possible that a pressure minimum can be found in the center of a rotation, it is not necessary. As a result this method is unsuitable for identifying vortices in complex flows [4].

3.4.4 Sectional Swirl-and-Pressure-Minimum Scheme

This method traces lines of pressure minima under a swirl condition to find the axis and the core of a vortex. It then visually represents these as so-called vortex skeletons. The idea is that as Reynolds numbers increase, the radius of the vortex cores decrease, therefore, if the vortex is sufficiently thin it can be represented by its central axis, and the core can be disregarded.

The vortex skeleton can be constructed in different ways. One such way is to trace the lines of sectional pressure minimum. The pressure minimum search begins in planes which are either normal to the vorticity or to the eigenvector associated with the smallest eigenvalue of the pressure Hessian. For strong slender vortices the results of both methods are comparable, as the planes are more or less parallel.

Because swirling motion is not always associated with a sectional pressure minimum, a condition is added to make sure that there will be swirling.

Consider an arbitrary point (x_1, x_2) in a flow. The velocity at this point is projected onto a plane which together with a third direction forms a Cartesian coordinate system moving with the velocity at that point. In this plane of reference the velocity is written as

$$\mathbf{u} = W_{ij}\mathbf{x}.$$

The topological structure of the streamlines in the vicinity of this point is characterised by the sign of the discriminant of the matrix W_{ij},

$$D = \frac{1}{4}(W_{11} - W_{22}) + W_{12}W_{21}$$

For a plane of arbitrary orientation the condition is defined as $D(\theta, \phi) < 0$. This results from rotating the Cartesian coordinate system. The angles (θ, ϕ) are given by the direction of the third eigenvector of the pressure Hessian [13].

3.5 Summary of Methods for Vortex Identification

- Methods based on the Velocity Gradient Tensor

  Q-criterion Looks at the second invariant of the velocity gradient tensor, Q. A vortex is defined as areas where $Q > 0$. Essentially this means a vortex is a connected region where the antisymmetric component of ∇u, that is the vorticity tensor, dominates over the symmetric one [9].

  Δ-criterion A vortex core is a region of space where the vorticity is sufficiently strong to cause the rate-of-strain tensor to be dominated by the rotation tensor, i.e. the velocity gradient tensor has complex eigenvalues. Whether the eigenvalues are complex can be determined by looking at the sign of the discriminant, Δ [3].

  λ_2-criterion This method is based on searching for pressure minima across the vortex, by taking the gradient of the Navier-Stokes equations and decomposing it into symmetric and antisymmetric parts [11].

  Swirling-strength Criterion Using the imaginary part of the complex eigenvalue of ∇u to visualise vortices and quantify the strength of the local swirling motion inside the vortex. The method is based on the Δ-criterion and identifies local strength on the local plane of swirling [21].

  Enhanced Swirling-strength Criterion The idea is to approximate the measure of the non-local orbital compactness based on local analysis of time-frozen flow fields. Using the ratio $\frac{\lambda_c r}{\lambda_c i}$, called the inverse spiralling compactness. A vortex is then defined as an area where the strength or rotation (swirling strength) is larger than a given threshold, and the orbital compactness is smaller than another threshold [2].

  Triple Decomposition A vortex is defined as a connected fluid region with a non-zero magnitude of the residual vorticity. The triple decomposition of ∇v aims to extract an effective pure shearing motion, so-called residual vorticity [14].

- Methods that rely on Vorticity

  These methods differ from those presented above in that they all calculate the vorticity and then attempt to visualise their findings in different

ways. In this sense they are all the same identification method, but different visualisation methods. The inability to distinguish between shear rotation and swirling motion is therefore something they all suffer from.

Vorticity Magnitude $|\omega|$ The method fails in boundary walls and cannot distinguish between shear rotation and swirling motion. The structure of the isosurfaces of vorticity magnitude varies with threshold. As a result this is a subjective method due to the arbitrary choice of threshold.

Vorticity lines The method is generally chaotic in three dimensions. Furthermore it is topologically and structurally unstable, as well as unable to represent the strength of vorticity [16].

Kinematic vorticity number N_k This method measures the quality of rotation. N_k is a pointwise measure of $|\omega|$ non-dimensionalised by the norm of the strain rate. N_k does not discriminate between vortices with small and large vorticity [19].

- Lagrangian Methods

Direct Lyapunov Exponents Using direct Lyapunov exponents (DLE) to identify Lagrangian coherent structures. The DLE is used as a measure of the separation (or attraction) of particles that start off nearby. This way attracting material structures (corresponding to structures seen using flow visualisation in experiments) can be found. This method is computationally expensive, as it requires the integration of particle trajectories [6].

M_Z **criterion** Looks at the fluid trajectories in thee dimensional incompressible flows. By looking at the resticiton of the strain acceleration tensor, defined as $\bar{M} = \partial_t \bar{S} + (\nabla \bar{S})\bar{v} + S(\nabla \bar{v}) + (\nabla \bar{v})^T \bar{S}$, to a zero strain cone Z it defines vortices as sets of fluid trajectories with indefinite M_Z. Physically this can be interpreted as "a material region where material elements do not align with subspaces that are near the eigenspaces of the rate of strain" [8].

- Other Methods

Closed or Spiralling Streamlines Spiral curves by observer moving with the vortex. Not Galilean invariant. Does not work for highly undsteady flows as they do not allow particles to complete a full rotation. Also as we do not know where the vortex in question is a priori we cannot place an observer in the path of the vortex. This is a non-local method [15].

Pressure Minima Works well for two-dimensional flow. The idea that a pressure minima can be found along the axis of the vortex is not necessarily true for unsteady, viscous or three-dimensional flow. Not appropriate for systems in which many vortices coexist. Arbitrary choice of pressure threshold.

R-definition Vortices here are considered to be material tubes of low particle dispersion. Non-local analysis introduces the idea of vortices

as structures. The particles inside a vortical structure show small variations in their relative distance even when following completely different trajectories. A vortex is defined as the region comprized of pairs of particles with R less than a threshold value [4].

Sectional Swirl-and-Pressure Minimum Scheme The method constructs vortex skeletons by tracing the lines of sectional pressure minimum. The swirl condition ($D(\theta, \phi) \geq 0$) where D is the discriminant of the velocity gradient tensor projected on a plane (so-called plane of swirling) [13].

4 Vortex Identification Directly from Velocity Field Information

4.1 Introduction to the Idea

This method for identification of vortices looks directly at the velocity field of two-dimensional planes. It builds on the simple idea that the direction of the flow around the center of rotation will have opposite signs on either side of the vortex. A first version of this method was tested, with surprisingly good results by just looking at the velocity components in one direction: perpendicular to both the direction of the flow and the expected axis around which the vortices would be rotating. A problem with only looking in one direction is however that the method is unable to distinguish between vortices and shear forces. To address this problem, and furthermore in order to narrow the definition of the vortex, the method was generalised to searthatch at the velocity components in two directions, thus attemtping to span the entire plane of rotation.

The method only searches planes, but by looking at the three principal orthogonal directions all possible planes of rotation are taken into account. This allows the method to work in three dimensions.

By analysing the velocity field information of the nearest neighbours of the point we are working with, this method traces the centre of rotation of the vortex. It does not however offer a solution to the problem of how far from the axis the vortex extends. An attempt to solve this is done by extending the axis to include the points with a common rotation around the center.

4.2 Description of the Method

The three-dimensional domain can be reduced to two dimensions because any arbitrary plane of rotation can be described by searching three orthogonal planes. Using a simple two-dimensional search for each plane therefore provides all the information necessary to locate the vortices. The final version superimposes information from different planes to create a three-dimensional result.

This method relies on a change of frame of reference. The necessary frame should be moving in the direction of the flow with the average flow velocity. To get to this frame from the "laboratory" frame the average flow velocity is calculated and subtracted from the matrix storing the velocity component in that direction.

Once a plane has been selected the algorithm carries out a number of steps described below.

4.2.1   Searching Algorithm

1. A signum operation is carried out on the matrices containing the velocity components in the directions that span the plane.

2. For each point in the plane the 4 neighbouring points are selected. See Figure 3. On each line only one velocity component is considered, as the figure shows when looking at either side of the point in the z-direction we are only interested in the velocity component in the x-direction.
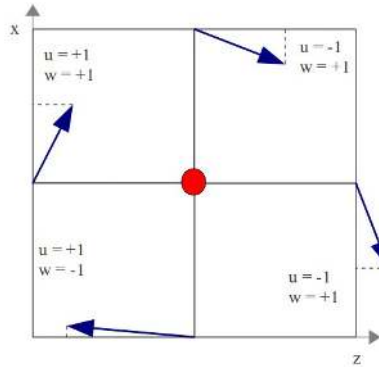

Figure 3: Figure showing what velocities the algorithm looks at for each point. The numbers represent the sign of the velocity components in the x- and z-directions for each point, **u** and **w** respectively

3. If the sum of the signum values of the velocity matrix in the relevant directions for the neighbouring points is zero a vortex centre is likely present.

4. An extra check is made to make sure the directions entail a rotation as there are two situations where the sum of the signum values can be zero, see Figure 4.
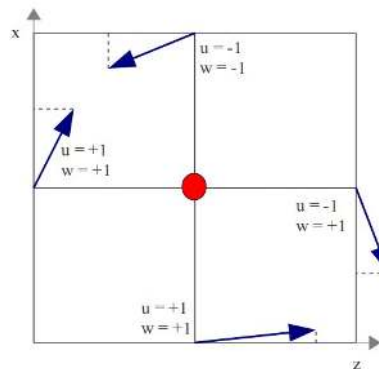
Figure 4: Figure showing a possible velocity profile leading to a "false vortex centre".

The situation in Figure 4 is clearly shear and not vortical motion. The check is done by checking the sum of the signum values for the upper and left points. If $sgn(u_{left}) + sgn(w_{up}) = 0$ the point is discarded.

5. A point is defined as belonging to a vortex centre if

$$sgn(u_{left}) + sgn(u_{right}) + sgn(w_{up}) + sgn(w_{down}) = 0$$

and

$$sgn(u_{left}) + sgn(w_{up}) \neq 0$$

6. For the points that fulfill the above criteria the strength of the vortex centre is calculated as the sum of the absolute values of the velocity components in the relevant directions. That is

$$strength(\mathbf{x}) = |(u_{left})| + |(u_{right})| + |(w_{up})| + |(w_{down})|$$

4.2.2 Growth Algorithm

The algorithm described above will find the smallest scale of rotation that can be identified in a given grid. A method to allow the core to "grow" from this centre is described below. This attempts to extend the parts of the domain and determine a cutoff that is not dependent on a predetermined threshold. The method works as follows:

1. The initial algorithm is carried out and every point inside a vortex is marked in the signum velocity matrices with a zero.

2. Every point in the plane is checked in the same way as the initial algorithm except when a zero is encountered. If a neighbouring point has a zero the algorithm will look past that until it reaches the first non-zero point in that direction. See Figure 5. If a point is found to qualify as a vortex the signum matrix is updated with new zeros.
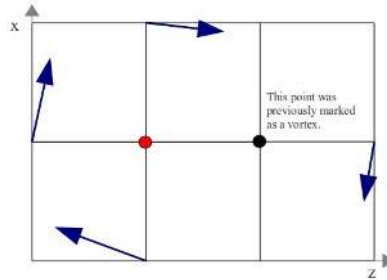

Figure 5: Figure showing what happens when a zero is encountered.

3. Step 2 is carried out a predetermined number of times, or until no new points are added.

4. The strength at each point is calculated by the searching algorithm. However when plotting the results, the strength is multiplied by a constant k, such that $0 \leq k \leq 1$. The constant is also raised to the power of the number of iteration we are plotting, for example in iteration number 2: $strength = strength \times k^2$. This way the size of the dots plotted will decrease as we move away from the centre even if the velocities increase.

4.2.3 Superposition of Results for Three-Dimensional Data

In order to use this method in three-dimensional data, the algorithm is applied to a large number of planes: the three principal planes for each point in our domain. Given that the actual data used in this thesis is obtained from numerical simulations performed in cartesian grids it is simple to look at every plane in the simulated data. Any arbitrary plane of rotation can be found using this method, as it can be expressed as a sum of rotation in the three cartesian planes. The method essentially performs an orthogonal decomposition of any arbitrary rotation.

The methods described above are then carried out for each plane. The results are stored in matrices with all the coordinates to the points where rotation was found and a vector with the strengths at all points. Each plane orientation has a matrix and a vector, allowing us to visualise the planes of rotation in the images produced.

We define the strength of rotation at each point to be given by the largest strength. That is, if a point has rotation in two planes, the strongest rotation will be given as the strength at that point.

4.3 Visualisation of the Results Obtained using this Method

The results from this method are visualised in two- or three-dimensional space as a set of dots. The size of the dot is determined by the strength of the vortex at that point. The colour of the dot is also connected to the strength at the point, while the colour of the edge marks what plane the rotation is found in.

While this visualisation is satisfactory in two-dimensions, and even in simpler three-dimensional cases, it becomes cluttered when the complexity of the flow increases. Small strength rotations add a lot of "noise" to the solution set making it more difficult to identify relevant structures. To minimise this problem a threshold has been added when visualising the results. This means that only rotations of a certain strength and higher are plotted in the solution.

The thresholds have been determined in different ways, generally the mean strength was used as a threshold, however in some cases (especially the turbulent ones) this proved to be too high, so a constant multiplied by the minimum strength was attempted instead.

Another attempt to make the vortical structures extracted using this method clearer has been to join the dots with lines. In this case the thickness of the lines is determined by the strength of the points it is connecting. The lines are only plotted for points that have a short Euclidean distance between them, i.e. neighbouring points with rotation.

4.4 Results

4.4.1 Wake of an Infinite Cylinder

As this case is the simplest among the data it was used to test if the results differ depending on how fine grid resolution is.

It was also used to check what kind of results can be obtained using the growth method. The method was run until it stopped on its own, and different number of iterations were tested. The decay constant in the growth method was chosen after trying several different values to get the clearest possible visualisation. The decay constant used in these results is 0.8 for both the coarse and the fine grid.

To aid in determining whether the results seem viable or not the velocity field in the plane being studied is plotted in the same figure, along with the area that is classed as a vortex core by the λ_2 method: λ_2 is less than zero. Zero has been chosen since it is the standard threshold in the definition of the λ_2 method. In practice, however, different thresholds are used to provide better visualisations. The darkened area in the images shows which areas are identified as a vortex core by the λ_2 method.

Coarse Grid
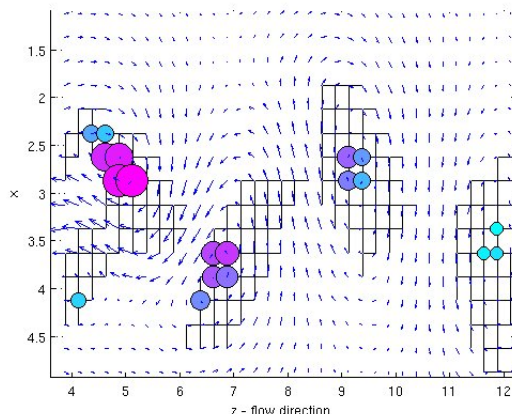
Figure 6: Results of the searching algorithm compared to the λ_2 method and the velocity field.

As we can see in Figure 6, the searching algorithm finds the centers of rotation to be inside the areas designated by the λ_2 method. As expected the centers of rotation can be found in the core of the vortex. In Figures 7 and 8 the growth algorithm has been used. After two iterations we can see that the size of the core from the λ_2 method is comparable to what is found using the direct method for most of the vortices. Finally, allowing the growth method to run until it stops itself (this requires 14 iterations) results in some of the vortices growing into each other. We can also see that the core grows unevenly in the different directions.
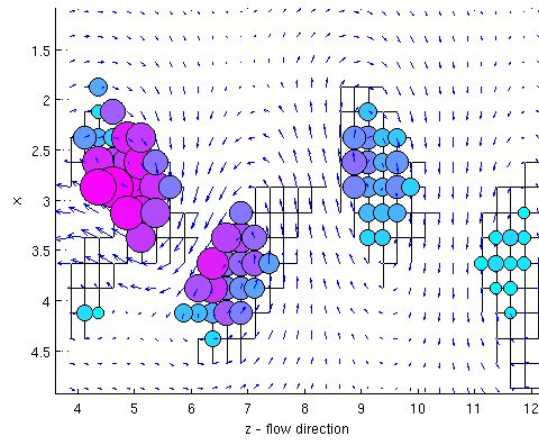
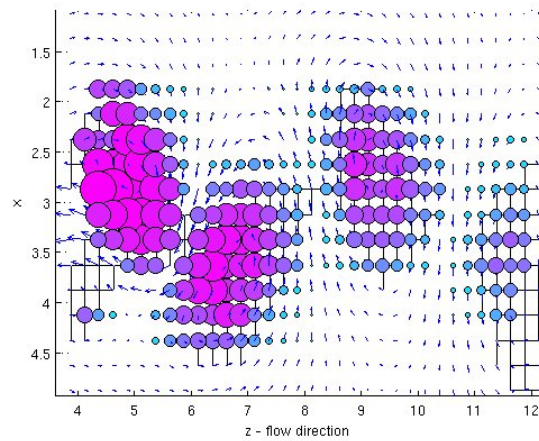Figure 7: Results after allowing the growth algorithm to run twice.

Figure 8: Results after allowing the growth algorithm to run until it stops on its own.

Fine Grid

On the fine grid the results are quite similar. Both methods find a similar number of points when only using the searching algorithm. This suggests that in a finer grid we identify a smaller part of the vortex core as its center. More iterations are required before the method stops itself (22 in this case). The areas considered to be vortices are more rounded with this method than what the λ_2 method obtains. The decay constant may be too low for the fine grid when letting the growth method run until it stops itself.
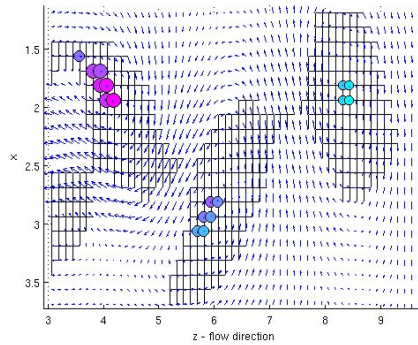
Figure 9: Results from the searching algorithm in the fine grid resolution.
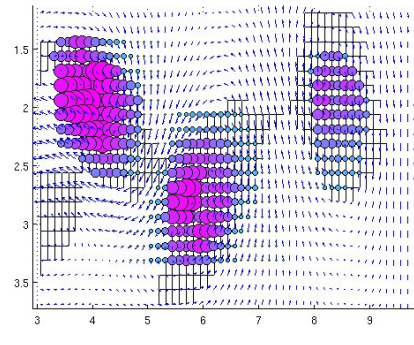
Figure 10: Results after allowing the growth algorithm to run until it stops on its own on the fine grid.

4.4.2 Laminar Wake of a Sphere: Hairpin Vortices

This is the simplest three-dimensional case as the wake of the sphere is laminar. Single vortices in this case rotate in different planes as the vortex is bent into the shape of something like a hairpin. In Figure 11 we can clearly see three hairpin shaped vortices among some smaller structures.
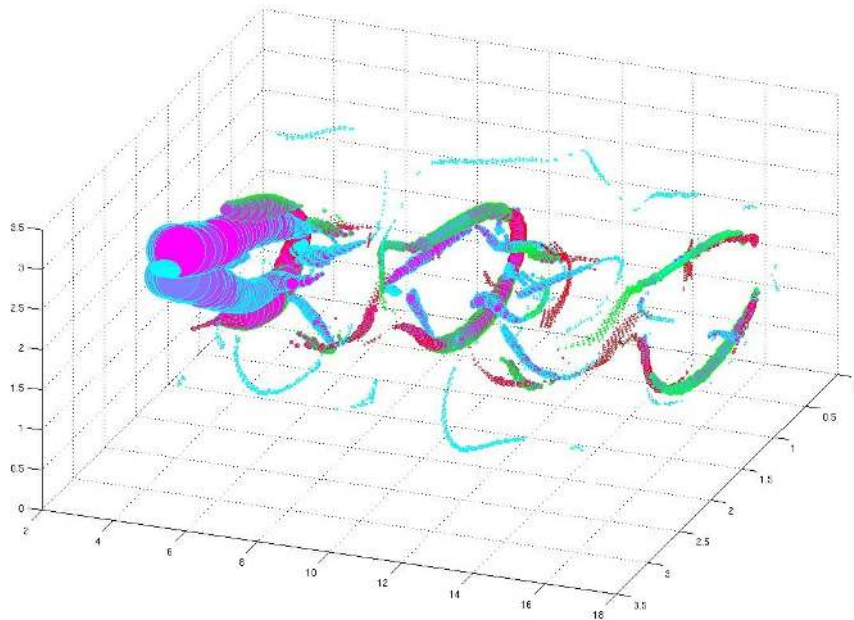
Figure 11: Visualisation showing all the points around which rotation can be found in the laminar wake of a sphere.

The growth method was also used with this data set. The results with a predetermined number of iterations are shown below. We can see in Figure 12 that it becomes difficult to make out the details when several structures are close to each other if too many iterations are used.
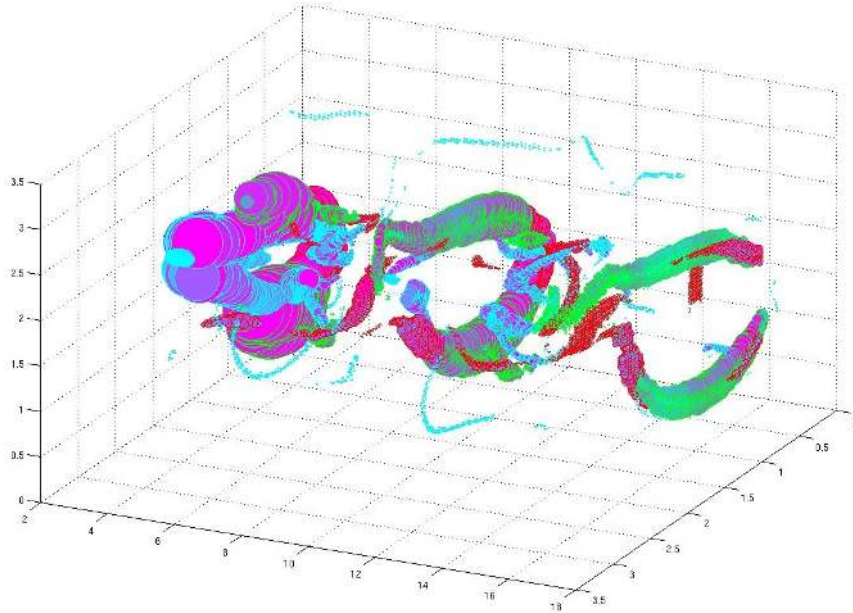

Figure 12: Visualisation showing all the points around which rotation can be found in the laminar wake of a sphere after three iterations of the growth method.

A threshold was introduced when creating the visualisations to make it easier to see how the larger structures behave. The threshold is set to 0.02, which is the mean strength for this case. While having a zero-threshold does not make these results hard to read in this case, as can be seen in Figure 11, it is likely to be worse for more complex cases. Also, when running the growth method, having too many points with very low strength slows the method down and makes the results much harder to read, see Figure 12.

A close up to the second hairpin can be seen in Figure 13 with different combinations of threshold and growth iterations. We can see that by adding a threshold the hairpins become clearer, by making sure weak rotations are not plotted. However, when examining the close up with a zero threshold we get more detail, and we can even see something that looks like a smaller hairpin growing out of the bigger one. This is not visible in the close up with a threshold and no growth but can be guessed at in the image with three growth iterations.
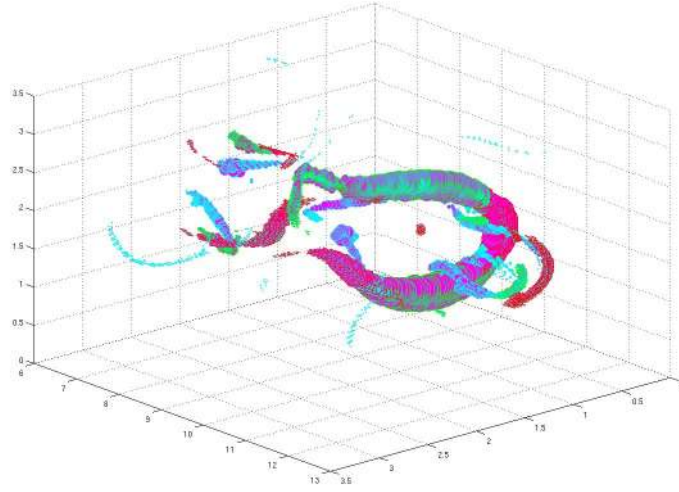
(a) Two growth iterations and 0 threshold
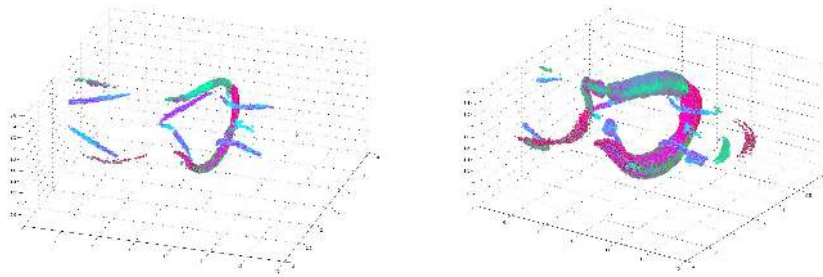
(b) Search algorithm with a 0.02 threshold   (c) Three growth iterations, 0.02 threshold

Figure 13: A close up of the second hairpin vortex with different combinations of threshold and growth iterations.

4.4.3   Turbulent Wake of a Sphere

The turbulent wake of a sphere is much less ordered than the laminar one, as can be seen in Figure 14. Growth iterations were attempted but none of the results were an improvement to what can be seen just from the search algorithm. As we can see, there are very many structures, and it is difficult to see individual ones in the mess.
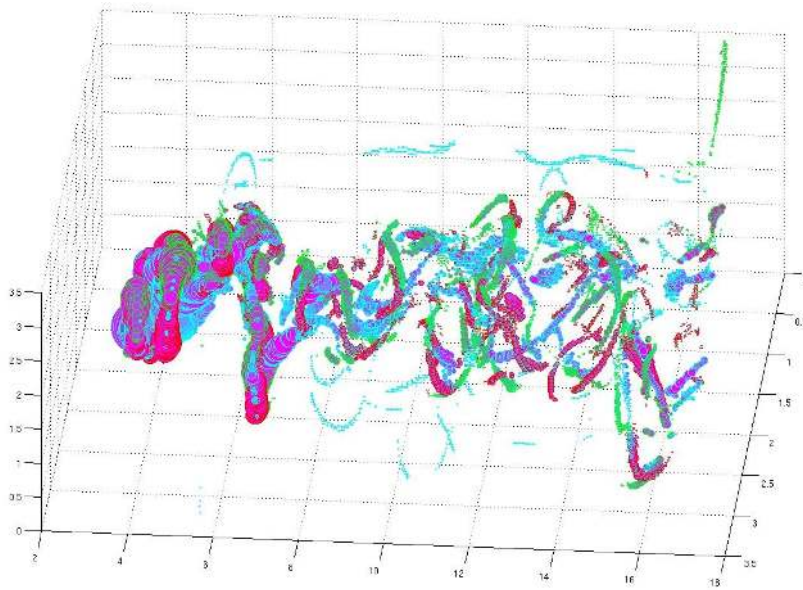
Figure 14: Turbulent wake of a sphere, zero threshold and no growth iterations.

However, some of the structures are similar to what was seen in the laminar case. At around z = 6 we can see what strongly resembles a hairpin vortex of the type seen in the previous case. Figure 15 shows a different angle of the same results, where we can see the structure more clearly.
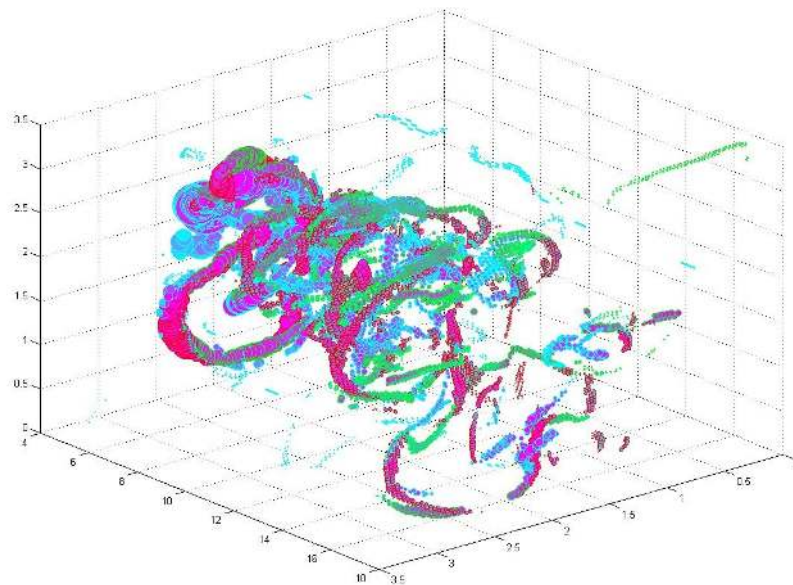

Figure 15: Turbulent wake of a sphere, zero threshold and no growth iterations.

An interesting observation is that after that structure the wake consists of smaller, weaker structures, and it is narrower than before that point. This can be very clearly seen when looking at the results where a strength threshold has been added.
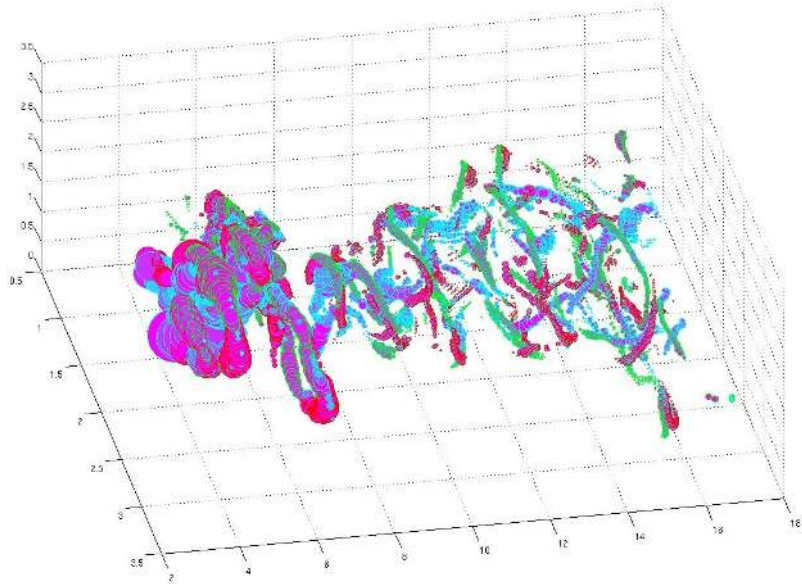

Figure 16: Turbulent wake of a sphere, threshold = 10*min(strength) and no growth iterations.

There is also a qualitative difference in this case when comparing to some results obtained with the λ_2 method, as seen in Figure 17. After the structure at z = 6 discussed above, the wake is made up of weaker structures threaded amongst each other. However when looking at the λ_2 results it seems like the smaller, thinner vortices recombine to make a larger structure near the end of the computational domain.
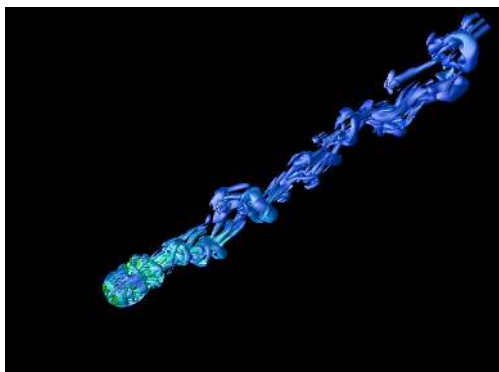

Figure 17: Vortex identification using λ_2 isosurfaces

4.4.4 A Jet

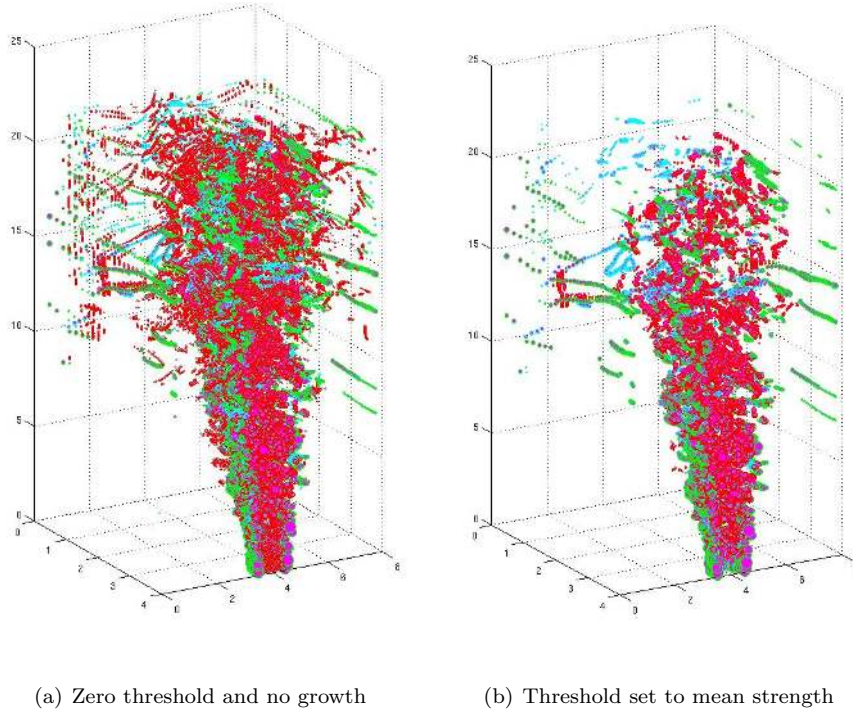(a) Zero threshold and no growth   (b) Threshold set to mean strength

Figure 18: Vortical structures in a jet

In Figure 18 we can see that the searching algorithm finds a lot or points with rotation. The results with no threshold fail to give us much information, other than that the results have the expected shape. However, once a threshold is added we can start seeing some more details. The first observation that can be made is that the rotation in the outer edges of the circular cross section is generally in the planes perpendicular to the plane in which the cross section lies, while the rotation inside of the jet is dominated by structures rotating around an axis in the direction of the flow.

The results are more interesting when looking at a close up of the flow closest to the nozzle. Figure 19 shows some results. Here we can see that closest to the nozzle all the rotation is found in the planes normal to the cross-section of the nozzle. However it quickly changes and structures rotating in the xz-plane (the plane of the nozzle) appear. These are fairly long, and have a helical shape. No vortices can be found in the volume directly above the nozzle itself. All the structures are formed at the edges.
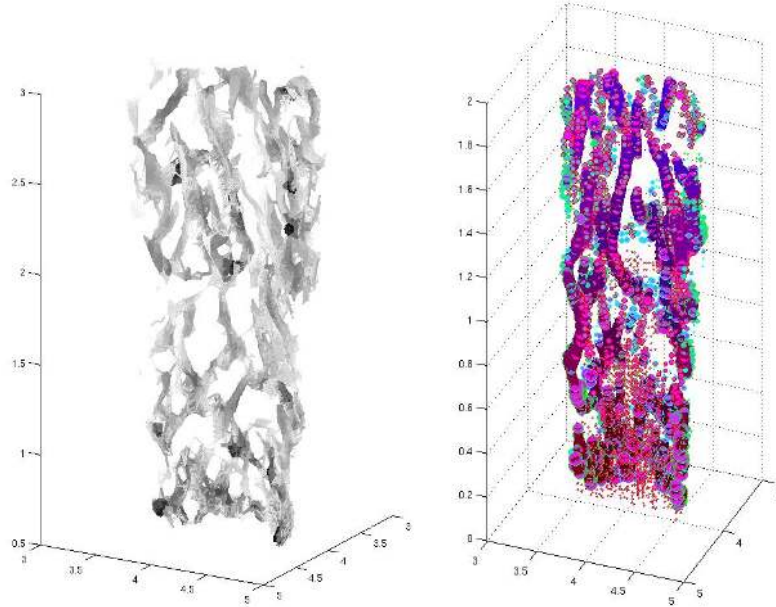
(a) Lines joining the points with rotation. Darker shades of grey represent stronger rotation

(b) Points showing vortical motion with a zero threshold with lines traced over areas with strength greater than the mean

Figure 19: Different views of the vortices found near the exit of a jet nozzle

4.5   Evaluation of the Method

The first thing to note about this method is that it is not Galilean invariant. It requires the selection of a suitable frame of reference and different results are received if the frame of reference is changed. This is clearly a weakness, especially if the method is intended for use in flows where the "predominant flow direction" is not clear, making it difficult to select the suitable reference frame.

That said, the simplicity of the method makes it attractive to implement, and the vortices identified using it are in agreement with our intuitive understanding of a vortex. It is also computationally inexpensive as no multiplications, gradients etc are required. Also, the searching algorithm can be potentially optimised by having a less extensive search.

However, some arbitrary tresholds are still in place. The most evident ones are a) the number of growth iterations if the extension of the core want to be increased, and b) the rate of decay in the strength of the later iterations. The choice of the measure of strength is in itself arbitrary, as it is defined to be the sum of the magnitude of the velocity components we search out in a neighbourhood of a given point. For example, when extending the core to more points the strength of the center could be defined as the sum of all the strengths

34

in that core, instead of just using the closest neighbours.

The results obtained using this method are also grid dependent. The smallest structure that can be found is determined by how fine the grid is. Also, if a vortex is assumed to be a structure having a certain diameter, searching in a fine grid would find a smaller percentage of the structure.

It is also clear that while visualising using points in a three-dimensional space works surprisingly well, it would be more appropriate to use surfaces instead, similar to those obtained from the λ_2 method. This has not been implemented due to time constraints.

A further improvement to the visualisation would be to include the direction of the rotation. This can be done by looking at the vorticity vector at each point marked as a vortex, as this would give the rotation direction in itself.

A more visually appealing visualisation would also be helpful, for example encasing the structures in surfaces resembling the λ_2 visualisation in Figure 17 instead of presenting them as clusters of points. Attempts to alternative visualisation methods can be seen in Figure 19 where a combination of lines and points has been used, these are however costly in memory and are therefore difficult to attempt with the whole domain.

5 Using the Direct Lyapunov Exponent to Calibrate the λ_2 Method

As described in the Overview of methods, the direct Lyapunov exponent is a measure of the separation between neighbouring particles after a certain period of time. The idea being that particles in a coherent structure will have little tendency to move apart from each other, while particles not belonging to the structure will move away quickly. It is similar to the R-method, and is non-local in nature.

As we have seen before, one of the main difficulties in identifying vortices is finding the edges of a vortex. Most of the methods we have seen rely on setting an arbitrary threshold for visualisation purposes. However, the Lagrangian methods, and especially the use of the Direct Lyapunov Exponent have a strength here, being that regardless of integration time, the edges are found to be in the same place. The main difference attained through using different integration times is how much detail of the different structures can be resolved [18, 6].

This of course invites the idea of combining an Eulerian method, such as the λ_2 method, with the direct Lyapunov exponent, and use the DLE method to locate the edges of a vortex together with an Eulerian method to find the core of the vortex. Further one can look at the λ_2 values at the edges found by the DLE method and set that as a threshold. The λ_2 method can then be used to identify vortices that will extend to the edges found by the DLE method. This means that the DLE method only has to be run once to calibrate λ_2 therefore decreasing computational cost.

Finding a threshold value using this method means that the threshold would no longer be arbitrary. It is likely that different cases will have different thresholds. And even within one frame it is possible that different vortices will have different λ_2 values on the boundaries. A suggestion is to choose the threshold

by averaging the values found at the boundaries.

To test if this idea is viable, a DLE method to locate lagrangian coherent structures is implemented and tested on the infinite cylinder case. This means that the method will only be used in two dimensions for this thesis. If sharp edges can be found using this method, the λ_2 values at those points will be extracted to attempt to find a threshold value.

5.0.1 Implementation of DLE Method

The DLE method is implemented in two dimensions. As a result only one plane is studied at a time, and therefore velcity components in the direction normal to the plane are not taken intp account. This will likely introduce an error to the solution, because any separation (or attraction) of particles in the y-direction will be unaccounted for.

The implementation of the method can be described in the following steps:

1. Once the velocity data for a plane has been loaded it is refined using linear interpolation. This is important for the resolution of the scalar field. In this case the grid is refined by 2^3 in each Cartesian direction. In the cases where different time frames are used, time is also interpolated to 5 times shorter steps. For a discussion of the accuracy of using refined numerical velocity data see [7].

2. Each point in the new grid is viewed as a particle, and its trajectory is integrated over a certain time. Explicit Euler is used as a time-stepping method. There are two versions of this, one integrates through physical time, looking at other different time frames. The other uses the instantaneous data in every "time-step". This is similar to the approach described in the R-criterion [4] where we imagine the flow is frozen at a point in time. This should make the results more comparable to what the λ_2 method provides as they are only based on instantaneous data. The time integration can be done either forward or backward in time.

3. Once the particle trajectories have been calculated every particle, $\bar{x}$ is viewed with a neighbour $\bar{y}$ at time t_0 and a differentiation is carried out as follows

$$\frac{d\Phi^T \bar{x}}{d\bar{x}} = \begin{bmatrix} \dfrac{y_x^T - x_x^T}{\delta x} & \dfrac{y_z^T - x_z^T}{\delta z} \end{bmatrix}$$

That is, the change in distance between them in the x and z directions compared to their initial separations.

4. When the differentiation has been carried out for every point (particle pair) the Lyapunov exponent can easily be calculated from the definition

$$\sigma_{t_0}^T(\bar{x}) = \frac{1}{|T|} ln\sqrt{\lambda_{max}(\Delta)}$$

where $\lambda_{max}(\Delta)$ is the largest eigenvalue of $\Delta = \frac{d\Phi^T \bar{x}}{d\bar{x}}^* \frac{d\Phi^T \bar{x}}{d\bar{x}}$

36

5. Finally, the ridges in the scalar field sigma are located. These are defined to be the Lagrangian Coherent Structures in [18]. Following the method outlined in the same paper, ridges are located as follows

- Calculate the Hessian at each point

$$\begin{bmatrix} \frac{\partial^2 \Phi(x_1)}{\partial x_1^2} & \frac{\partial^2 \Phi(x_1)}{\partial x_1 \partial x_2} \\ \frac{\partial^2 \Phi(x_2)}{\partial x_1 \partial x_2} & \frac{\partial^2 \Phi(x_2)}{\partial x_2^2} \end{bmatrix}$$

- Calculate the gradient at each point
- Calculate the eigenvalues of the Hessian at each point. The eigenvector corresponding to the smallest eigenvalue direction is extracted, λ_{min}
- A new scalar field is created by calculating the inner product of the gradient and λ_{min} at each point.

Once the DLE field is plotted the boundaries of the vortices can be seen. An appropriate vortex is then chosen and its edge extracted. In this case the edge is extracted by choosing the points above a certain threshold. The λ_2 values at the edge are then studied and an attempt to chose a threshold based on this information is made.

5.1 Results

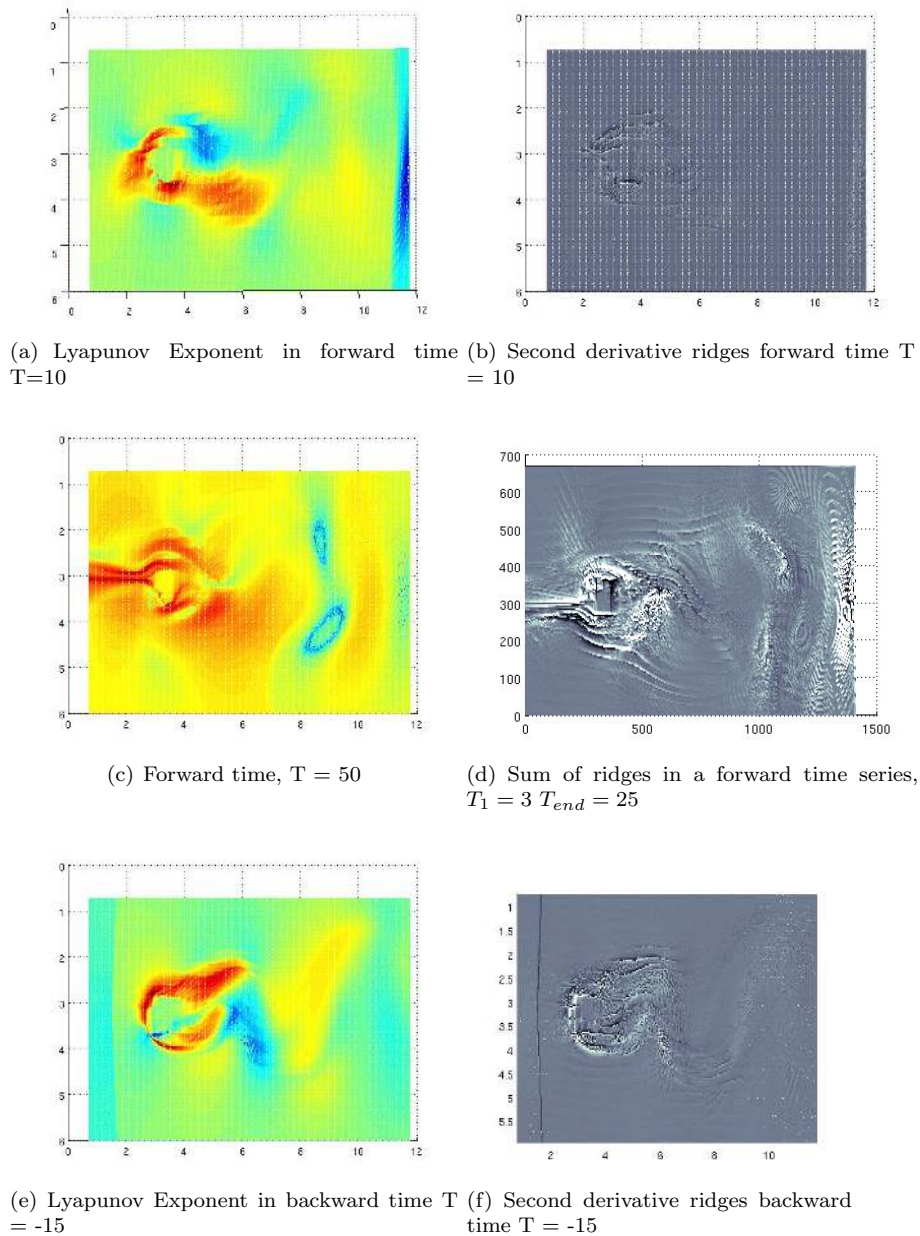### 5.1.1 Integrating through Physical Time

(a) Lyapunov Exponent in forward time T=10

(b) Second derivative ridges forward time T = 10

(c) Forward time, T = 50

(d) Sum of ridges in a forward time series, $T_1 = 3$ $T_{end} = 25$

(e) Lyapunov Exponent in backward time T = -15

(f) Second derivative ridges backward time T = -15

Figure 20: DLE method in forward and backward time for different integration times

These results are more difficult to interpret. According to [6] integration in backward time reveals vortices, since they are attracting Lagrangian Coherent Structures. Integration in forward time reveals repelling structures, which

38

means when a particle reaches the edge of one of these structures it cannot pass through. Therefore these should be boundaries through which little or no mixing occurs. In both cases, the Lyapunov exponent highlights areas of high shear as well as the structures we are looking for.

5.1.2 Frozen Flows

Looking at a time frozen flow should make it easier to compare with the instantaneous methods such as the λ_2 method and the method shown in the previous section. This is because we only look at the flow in that time instant, therefore we have the same amount of information as the instantaneous methods have. In order to calculate a Lyapunov exponent in this case we imagine that the particles are moving in a steady flow and follow their trajectories there. The results shown in Figure 21 are compared to the λ_2 method in the same time-frame.
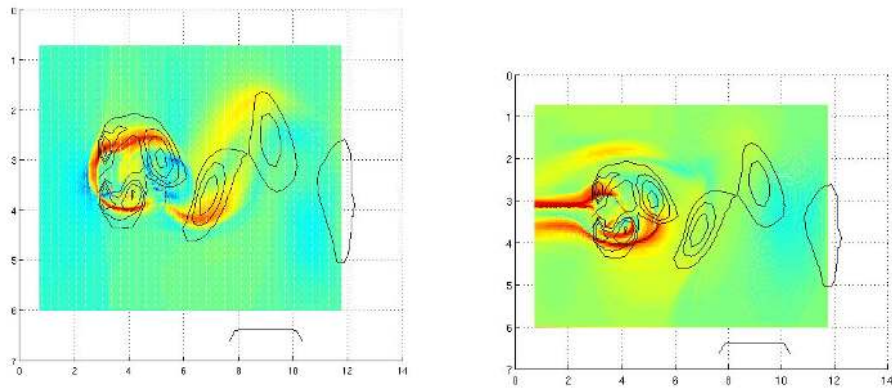

(a) Backward integration with pseudo-time t=- (b) Forward integration with pseudo-time t=300
150

Figure 21: Results of the DLE method with a frozen flow.

An interesting attempt is presented in Figure 23 where the velocity field was changed by subtracting the average velocity in the direction of the flow. The results are shown below with a plot of the respective velocity fields. The ridges are then calculated for each case. Notice that the altered case has a better correspondence to the λ_2 contours. See Figure 23.
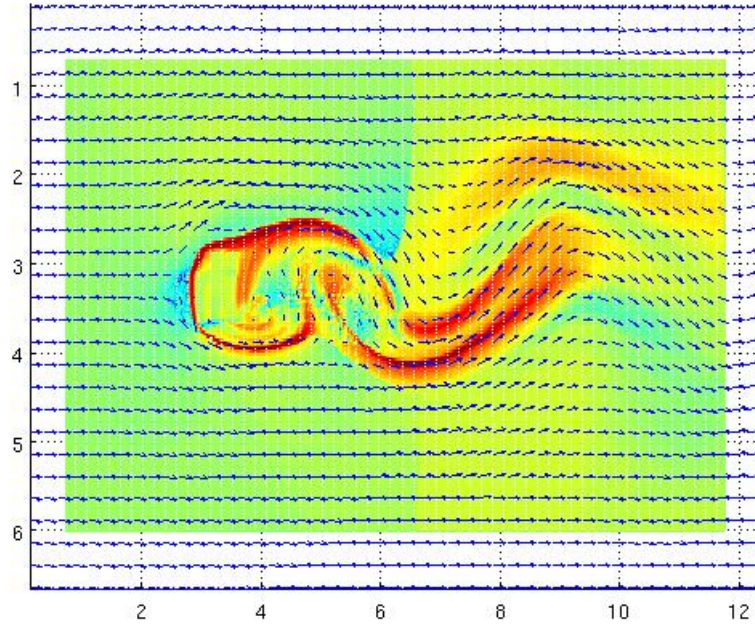
(a) Backward integration with actual velocity field, including a velocity field plot
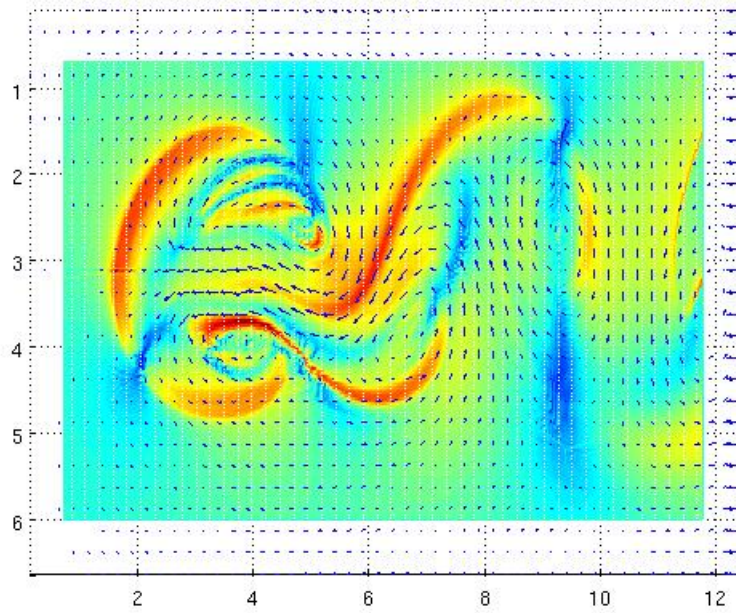
(b) Backward integration with altered velocity field, including a velocity field plot

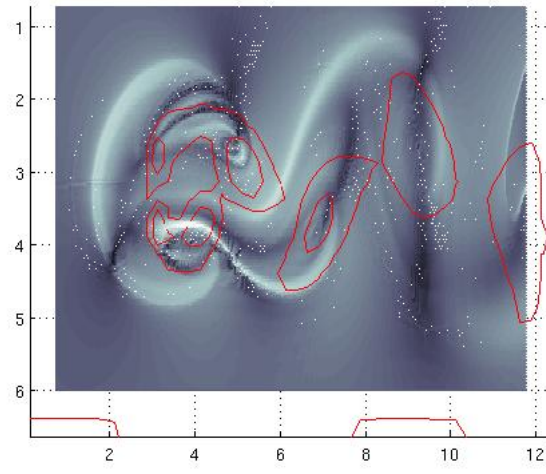Figure 22: Different results obtained by changing the velocity field

Figure 23: The Lyapunov Exponent for backward time integration t = -300 in the altered velocity and contours for $\lambda_2 = 0$ and $\lambda_2 = -0.5$
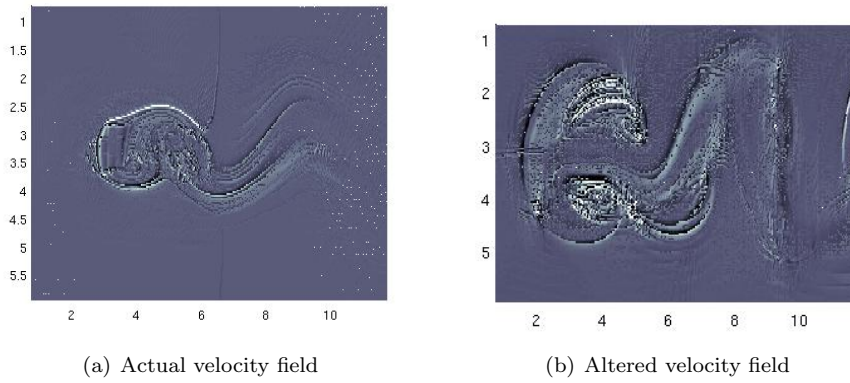

(a) Actual velocity field

(b) Altered velocity field

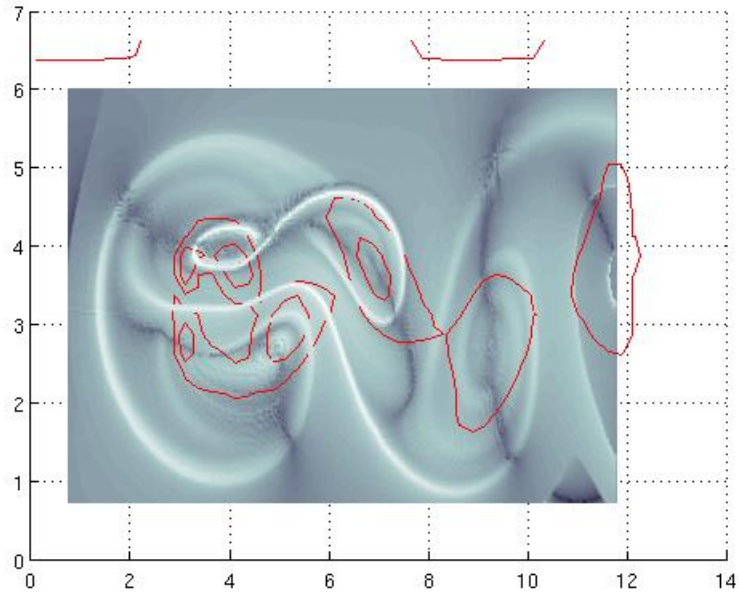Figure 24: Ridges from backward integration

Figure 25: Lyapunov exponent with t = -700 and λ_2 contours traced on it

From Figure 25 the edge to a vortex is traced. The edge we will be looking at is marked on a λ_2 field in Figure 26.
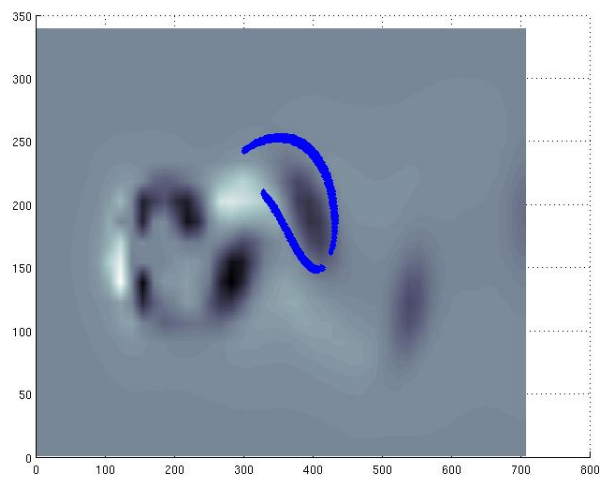

Figure 26: The edge we are looking at is superimposed on a plot of the λ_2 values in the domain

In Figure 27 we can see a plot of how the λ_2 values vary along the edge. The maximum is $\lambda_2 = 0.4797$, the minimum $\lambda_2 = -0.3168$ and the mean $\bar{\lambda}_2 = 0.0125$. It is evident that chosing a threshold is more complicated than simply finding the mean. A more detailed study of ways to optimise the choice of threshold based on the boundaries given by the DLE is necessary.

(a)   (b)
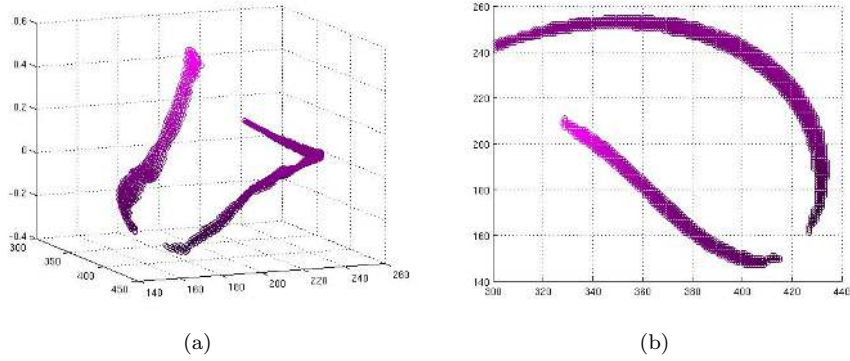
Figure 27: Different views of the variation of λ_2 along the edge of a vortex

(a) t = 5   (b) t = 10

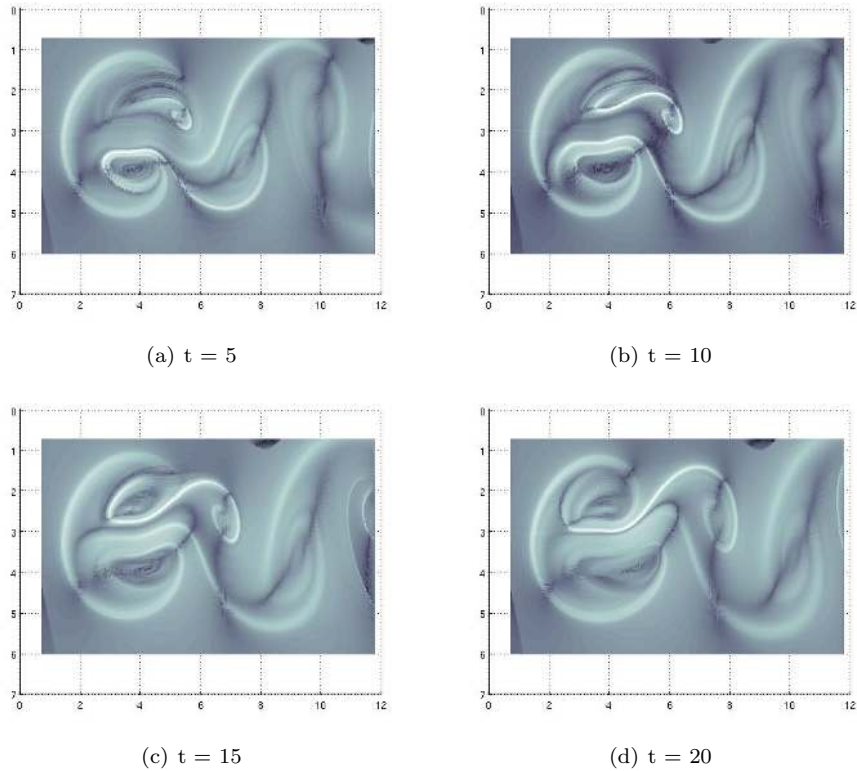(c) t = 15   (d) t = 20

Figure 28: Backward DLE with 500 iteration seen in different time frames

As seen in the results in Figure 28, a dark line consistenly can be seen through the vortices. This line is likely an area of high shear, which could potentially give more information on how the vortices will evolve in time. We would assume the vortices to be deformed along a line of high shear, and the line to rotate with the vortex until it is shed from the cylinder, which is in fact what we see in the results.

5.2 Evaluation

It is positive to see that the areas with negative λ_2 are found inside the boundaries of the DLE structures. The results indicate that the mean λ_2 value along the edge is an inappropriate way to get a value. In fact, calculating a single λ_2 threshold using the DLE boundaries is difficult due to the large variation of λ_2 values along the boundary. It would also be interesting to follow a single vortex in time to see how the relation between DLE boundary and λ_2 value evolves.

Choosing the boundary by setting a threshold is not ideal, but it is a good way to start studying what kind of values the λ_2 method finds in what look like clear boundaries in the DLE method. As can be seen in Figure 28 the same flow can have different DLE values in different time frames, making it difficult to use this method when looking at the time evolution of a flow. A better edge detection method could improve this part of the method. It could also be of interest to chose a narrower line as the edge. What is extracted using the threshold approach is quite thick, and therefore the λ_2 values vary even along the width of the line.

The DLE method is computationally very costly, and the errors introduced when using a small domain, like the one we have tested it on, are probably quite high (further work necessary). However it is still very interesting to find a less arbitrary way of chosing the threshold in the λ_2 method.

In this implementation particles that leave the computational domain are stopped at the boundary, this is likely to introduce a sizeable error into the computation, especially in the areas far from the center of the domain. Another error is introduced as the particles are allowed to travel through the cylinder, this means that the part of the domain up to the cylinder is highly innaccurate.

In order to study the line of high shear a longer computational domain could be of interest in order to follow a single vortex through its entire evolution in time.

6 Conclusion and Future Work

In this thesis we have presented an overview of methods that have been used, and still are used, for identifying vortices. The methods are presented shortly including the theory motivating the definitions given by each. An attempt was made to concretely present the advantages and disadvantages of the different methods. However, as the different methods are tested in different ways it is difficult to find concrete weaknesses and strengths for many of them.

A new method for vortex identification, using velocity field information directly, was presented and tested in four different simulated data sets. The results are in accordance with the intuitive expectations, including the more complex flows: a jet and turbulent wake of a sphere. The visualisation method used

in the tests (a plot of points in a three-dimensional domain) is sufficient for testing purposes but there is much room for improvement. It was seen that in the more complex flows the visualisations became cluttered, making it difficult to get a clear view of the structures identified. Other visualisation approaches were tested with good results, however they were not applied to a full result set due to computer memory constraints.

Finally, two of the methods presented in the overview were implemented and combined. The direct Lyapunov Exponent was used to identify edges of vortices in the laminar wake of a cylinder, a case with two-dimensional vortices. The aim was to use the edges found to calibrate the λ_2 method. By chosing a threshold for the visualisation based on the λ_2 values along the edge in the DLE method the subjectivity of the choice of theshold could be removed. However, it was found that the λ_2 values have a large variation along the edges in the DLE field, making it impossible to find a single λ_2 value that would result in matching edges.

However, it was gratifying to note that the $\lambda_2 < 0$ areas are generally found inside the DLE edges, meaning that using both methods can provide an answer to where the core of the vortex is as well as its extent. The DLE method also shows a set of dark lines that go through the vortices it highlights, see Figure 28. These are of interest as they may provide more information regarding how a vortex will be deformed in time.

There is much that can be improved upon and done in the future in this area. The combination of the DLE method with existing Eulerian methods is very interesting, due to the DLE method's ability to unambiguosly find an edge to a vortex. A three-dimensional implementation and testing in more complex flows is necessary to judge the potential of combining such methods.

References

[1] Beju, I. (1983) *Euclidean tensor calculus with applictions.* Revised and updated translation of "Tehnici de calcul tensorial euclidian cu aplicatii", Abacus Press 1983

[2] Pinaki Chakraborty, S. Balachandar, Ronald J. Adrian, 2005 *On the relationships between local vortex identification schemes* J. Fluid Mech., pp.189-214

[3] M. S. Chong, A. E. Perry, B. J. Cantwell (1990) *A general classification of threedimensional flow fields* Phys. Fluids A 1 , 765 (1990); doi: 10.1063/1.857730

[4] R. Cucitore, M. Quadrio, A. Baron, 1999 *On the effectiveness and limitations of local criteria forthe identification of a vortex* Eur. J. Mech. B/Fluids, 261-282

[5] Robert L. Devaney *An Introduction to Chaotic Dynamical Systems* 1986 The Benjamin/Cummings Publishing Company, Inc.

[6] M.A. Green, C.W Rowley and G. Haller (2007) *Detection of Lagrangian coherent structures in three-dimensional turbulence* J. Fluid Mech. (2007), vol. 572, pp. 111-120; doi: 10:1017/S0022112006003648

[7] G. Haller, 2002 *Lagrangian coherent structures from approximate velocity data* Phys. Fluids 14, 1851 (2002); doi: 10.1063/1.147449

[8] G. Haller, 2005 *An Objective Definition of a Vortex* J. Fluid Mech. 1-26

[9] J.C.R. Hunt, A.A. Wray, P. Moin, 1988 *Eddies, stream, and convergence zones in turbulent flows.* Center for Turbulence Research Report CTR-S88, pp. 193-208

[10] M. C. Irwin *Smooth Dynamical Systems* (2000) First published in 1980. World Scientific Publishing Co.

[11] Jinhee Jeong, Fazle Hussain, 1995 *On the identificaiton of a vortex* J. Fluid Mech., pp.69-94

[12] Jurgen Jost (2005) *Dynamical Systems. Examples of Complex Behaviour* Springer-Verlag Berlin Heidelberg 2005

[13] S. Kida, H. Miura, 1998 *Identification and Analysis of Vortical Structures* Eur. J. Mech. B/Fluids, 471-488

[14] Václav Kolář, 2007 *Vortex identification: New requirements and limitations* International Journal of Heat and Fluid flow 638-652

[15] H.J. Lugt, 1979 *The dilemma of defining a vortex* In *Recent Developments in Theoretical and Experimental Fluid Mechanics* (ed. U. Mller, K.G. Roesner & B. Schmidt), pp. 309-321. Springer

[16] Parviz Moin, John Kim, 1984 *The Structure of the Vorticity Field in Turbulent Channel Flow Part 1: Analysis of Instantaneous Fields and Statistical Correlations*

[17] Stephen B. Pope (2000) *Turbulent Flows* (1st Edition) Cambridge University Press

[18] Shawn C. Shadden, Francois Lekien, Jerrold E. Marsden (2005) *Definition and properties of Lagrangian coherent structures from finite-time Lyapunov exponents in two-dimensional aperiodic flows* Physica D 212 (2005) 271-304

[19] C. Truesdell, 1953 *The Kinematics of Vorticity* Indiana University.

[20] Donald F. Young, Bruce R. Munson, Theodore H. Okiishi, Wade W. Huebsch (2007) *A Brief Introduction to Fluid Mechanics* (4th Edition) John Wiley & sons Inc.

[21] J. Zhou, R.J.Adrian, S. Balachandar, T.M. Kendall (1999) *Mechanisms for generation coherent packets of hairpin vortices in channel flow* Journal of Fluid Mechanics, 387, pp 353-396 doi:10.1017/S002211209900467X